



**THE DEVELOPMENT OF NOVEL ORTHODONTIC
ADHESIVES CONTAINING STRONTIUM/CALCIUM
PHOSPHATE AND ANDROGRAPHOLIDE**

BY

MISS WIRINRAT CHAICHANA

**A THESIS SUBMITTED IN PARTIAL FULFILLMENT OF THE
REQUIREMENTS FOR THE DEGREE OF
MASTER OF SCIENCE IN DENTISTRY
FACULTY OF DENTISTRY
THAMMASAT UNIVERSITY
ACADEMIC YEAR 2021**

COPYRIGHT OF THAMMASAT UNIVERSITY

**THE DEVELOPMENT OF NOVEL ORTHODONTIC
ADHESIVES CONTAINING STRONTIUM/CALCIUM
PHOSPHATE AND ANDROGRAPHOLIDE**

BY

MISS WIRINRAT CHAICHANA

**A THESIS SUBMITTED IN PARTIAL FULFILLMENT OF THE
REQUIREMENTS FOR THE DEGREE OF
MASTER OF SCIENCE IN DENTISTRY
FACULTY OF DENTISTRY
THAMMASAT UNIVERSITY
ACADEMIC YEAR 2021**

COPYRIGHT OF THAMMASAT UNIVERSITY

**THAMMASAT UNIVERSITY
FACULTY OF DENTISTRY**

THESIS

BY

MISS WIRINRAT CHAICHANA

ENTITLED

**THE DEVELOPMENT OF NOVEL ORTHODONTIC ADHESIVES CONTAINING
STRONTIUM/CALCIUM PHOSPHATE AND ANDROGRAPHOLIDE**

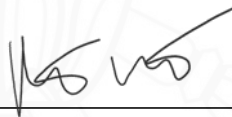
was approved as partial fulfillment of the requirements for the degree
of Master of Science program in dentistry (Major in Orthodontic Dentistry)
on August 31, 2021

Chairman



(Prof. Dhirawat Jotikasthira, FRCDS)

Member and Advisor



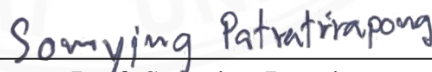
(Assoc. Prof. Piyaphong Panpisut, Ph.D)

Member and Co-Advisor



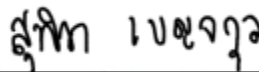
(Asst. Prof. Kanlaya Insee, FRCDS)

Member



(Assoc. Prof. Somying Patntirapong, DMSc.)

Member



(Asst. Prof. Sutiwa Benjakul, Ph.D)

Dean



(Assoc. Prof. Samroeng Ingiam, Ph.D.)

Thesis Title	THE DEVELOPMENT OF NOVEL ORTHODONTIC ADHESIVES CONTAINING STRONTIUM/CALCIUM PHOSPHATE AND ANDROGRAPHOLIDE
Author	Miss Wirinrat Chaichana
Degree	Master of Sciences
Major Field/Faculty/University	Orthodontics Faculty of Dentistry Thammasat University
Thesis Advisor	Assist. Prof. Dr. Piyaphong Panpisut
Thesis Co-Advisor	Assist. Prof. Kanlaya Insee
Academic Year	2021

Abstract

Objective: The progression of white spot lesions around orthodontic adhesives or brackets is the common esthetic concern during orthodontic treatment. This could be due to the lack of ion releasing and antibacterial actions of the current resin composite orthodontic adhesives to prevent dental caries. The aim of the current study was to prepare orthodontic resin composite adhesives containing strontium-bioactive glass nanoparticles (SrBGNPs), monocalcium phosphate monohydrate (MCPM), and andrographolide (Andro) to promote ion releasing and inhibitory effect on growth of *S. mutans*. Effects of increasing concentration of Sr/CaP (SrBGNPs + MCPM) and Andro on the physical, mechanical, and the growth of *S. mutans* of experimental adhesives were examined.

Materials and methods: The liquid phase contained light-activated methacrylate monomers. The powder phase contained silanated boroaluminosilicate glass, Sr/CaP (SrBGNPs + MCPM)(5 or 10 wt%), and Andro (5 or 10 wt%). The control formulation contained 0 wt% of additives. The powder and liquid phases were mixed with a powder to liquid mass ratio of 4:1. The degree of monomer conversion was assessed using FTIR-ATR (n = 5). Water sorption / solubility after immersion in deionized water for 4 weeks was determined (n = 6). Biaxial flexural strength (BFS) / modulus (BFM) at 24 h was assessed using a mechanical testing frame (n = 7). Enamel shear bond strength (SBS) and adhesive remnant index (ARI) were determined using the SBS testing jig (n = 5). The mineral precipitation in the materials was examined under SEM-EDX (n = 2). Ion release was assessed using ICP-OES (n = 3). The inhibition of *S. mutans* growth was determined by assessing the colony-forming unit (Log CFU/mL, n = 3). The commercial material (Transbond XT, Trans) was used as a comparison.

Results: The degree of monomer conversions of experimental adhesives (46 – 62 %) were higher than that of Trans (38 %). The additives reduced degree of monomer conversion, but the effect of increasing levels of Sr/CaP and Andro on the conversion was negligible. Rising the level of Sr/CaP increased water sorption whilst rising the level of Andro increased the water solubility of the materials. The additives reduced the BFS and BFM of the materials. The increase of Sr/CaP level showed minimal effect on the strength of materials. The addition of Sr/CaP enabled the precipitation of calcium phosphate apatite and the release of Ca, P, and Sr ions. Rising Sr/CaP level reduced log CFU/mL of *S. mutans* whilst the rising of Andro did not reduce the growth of *S. mutans*.

Conclusions: The additives reduced the mechanical properties of the experimental orthodontic adhesives. The increase of Sr/CaP level promoted desirable anti-caries actions such as ion release and inhibition of *S. mutans* growth. The increase of Andro level, however, reduced mechanical properties of the materials with no inhibition effect on the growth of *S. mutans*.

Keywords: Orthodontic adhesive, remineralization, bioactive glass, calcium phosphates, andrographolide

Table of Content

Abstract.....	5
Table of Content.....	6
Acknowledgement	9
List of Table	10
List of Figure	11
List of Abbreviation	15
Chapter 1 Introduction.....	18
Chapter 2 Review of literature.....	21
2.1 Orthodontic treatment.....	21
2.2 Orthodontic adhesive	21
2.3 Enamel demineralization / white spot lesion (WSL) due to fixed orthodontic treatment.....	22
2.4 The effect of the fixed orthodontic appliances on bacterial colonization.....	24
2.5 The modification of orthodontic adhesive to reduce and prevent initial caries lesions (white spot lesions)	25
2.5.1 Remineralizing agents	25
2.5.2 Antibacterial agents	28
Chapter 3 Statement of problems, objectives, and hypotheses	32
3.1 Statement of problems	32
3.2 Objectives.....	32
3.3 Research hypotheses	33
Chapter 4 Materials and methods	34
4.1 Materials preparation.....	34
4.2 Degree of monomer conversion.....	37
4.3 Water sorption (W_{sp}) and solubility (W_{sl})	38

4.4	Biaxial flexural strength (BFS) and biaxial flexural modulus (BFM).....	41
4.5	Shear bond strength (SBS) and adhesive remnant index (ARI).....	42
4.6	Mineral precipitation	46
4.7	Ion release	46
4.8	The inhibition of <i>S. mutans</i> growth	47
4.9	Statistical analysis	47
Chapter 5	Results	49
5.1	Degree of monomer conversion (DC)	49
5.2	Water sorption (W_{sp}) and solubility (W_{sl})	50
5.3	Biaxial flexural strength (BFS) and Biaxial flexural modulus (BFM)	51
5.3.1	Biaxial flexural strength (BFS)	51
5.3.2	Biaxial flexural modulus (BFM)	52
5.4	Enamel shear bond strength (SBS) and adhesive remnant index (ARI).....	54
5.4.1	Enamel shear bond strength (SBS).....	54
5.4.2	Adhesive remnant index (ARI)	55
5.5	Mineral precipitation	56
5.6	Ion release	58
5.7	The inhibition of <i>S. mutans</i> growth	59
Chapter 6	Discussion.....	61
6.1	Degree of monomer conversion (DC)	61
6.2	Water sorption (W_{sp}) and solubility (W_{sl})	62
6.3	Biaxial flexural strength (BFS) and Biaxial flexural modulus (BFM)	63
6.4	Enamel shear bond strength (SBS) and Adhesive remnant index (ARI).....	64
6.5	Mineral precipitation	65
6.6	Ion release	66
6.7	The inhibition of <i>S. mutans</i> growth	67

6.8	The summary of the additive effects of this current study was exhibited in the Table 6-1.....	68
6.9	Future works.....	68
6.10	Limitation.....	69
Chapter 7	Conclusions	70
Chapter 8	References	71



Acknowledgement

Firstly, I would like sincerely to thank my advisor Assist. Prof. Dr. Piyaphong Panpisut and Assist. Prof. Kanlaya Insee for their invaluable advice, guidance, and encouragement throughout my research.

Many thanks to the technical staff at the Medicinal Extract and Dental Biomaterials and Laboratory at Faculty of Dentistry, Thammasat University, for their training and technical assistance.

I also want to acknowledge Dr. Visakha Aupaphong for the invaluable guidance in performing the antibacterial test.

I would like to thank the Bureau of Dental Health, Ministry of Health, for providing scholarships to my master of science study.

Finally, I would like to thank my family for supporting and encouraging me to finish my master degree.

Miss Wirinrat Chaichana

List of Table

Table	Page number
Table 4-1 Chemicals used in this study.	34
Table 4-2 Formulation of the liquid component.	35
Table 4-3 The composition of the experimental orthodontic adhesives. The level of glass was reduced to maintain the total mass percentage of 100 wt%.....	36
Table 4-4 The information on ingredients of Tranbond XT light cure adhesive (3M Unitek, St. Paul, MN, USA as commercial control).	36
Table 4-5 Composition of the artificial saliva (grams per litre).	43
Table 5-1 Raw data of Ion release.....	58
Table 6-1 The summary of the additive effects.	68

List of Figure

Figure	Page number
Figure 2-1 Orthodontic white spot lesions (WSL) on enamel surfaces; these were adjacent to labial fixed orthodontic appliances (Chapman et al., 2010). Reprinted from <i>American Journal of Orthodontics and Dentofacial Orthopedics</i> , Vol 138-2, Chapman JA, Roberts WE, Eckert GJ, Kula KS, González-Cabezas C, Risk factors for incidence and severity of white spot lesions during treatment with fixed orthodontic appliances, Pages 188-194, Copyright (2010), with permission from Elsevier	23
Figure 2-2 QLF images: the dark areas are areas of demineralization (Al Maaitah et al., 2011). Reprinted from <i>American Journal of Orthodontics and Dentofacial Orthopedics</i> , Vol 2, Al Maaitah EF, Adeyemi AA, Higham SM, Pender N, Harrison JE, Factors affecting demineralization during orthodontic treatment: a posthoc analysis of RCT recruits, Pages 181-191, Copyright (2011), with permission from Elsevier	23
Figure 2-3 SEM images of plaque accumulation around the bracket. (a) Bonded tooth ligated with stainless steel wire (W) reveals abundant plaque deposition on excess composite, under bracket wings, and on and under the ligature wire, whereas sparse plaque is present on the enamel cervical to composite. The enamel-composite junction cannot be characterized due to the heavy plaque deposit. B, bracket wing; BB, bracket base; C, composite; E, enamel)(Sukontapatipark et al., 2001) Reprinted from Sukontapatipark W, El-Agroudi MA, Selliseth NJ, Thunold K, Selvig KA, Bacterial colonization associated with fixed orthodontic appliances, <i>The European Journal of Orthodontics</i> , 2001, vol 23(5), Pages 475-484, Copyright (2001) by permission of Oxford University Press	24
Figure 2-4 SEM images for composite (a) 0% CaP, (b) 10% CaP, (c, e and f) 20% CaP and (d) 40% CaP immersed in SBF for 1 week (Aljabo et al., 2016) Reprinted from <i>Materials Science and Engineering</i> , Vol 60, Aljabo A, Abou Neel EA, Knowles JC, Young AM, Development of dental composites with reactive fillers that promote precipitation of antibacterial hydroxyapatite layers, Pages 285-292, Copyright (2016), with permission from Elsevier	27

Figure 2-5 Chemical structure of Andrographolide (Andro) and related analogues (Jiang et al., 2009) Reprinted from <i>European journal of medicinal chemistry</i> , Vol 44(7), Jiang X, Yu P, Jiang J, Zhang Z, Wang Z, Yang Z, Tian Z, Wright SC, Larrick JW, Wang Y, <i>Synthesis and evaluation of antibacterial activities of andrographolide analogues</i> , Pages 2936-2943, Copyright (2009), with permission from Elsevier	30
Figure 4-1 Chemical agents and tools for liquid phase preparation: A. liquid agents, B. The 4-figure balance, C. magnetic stirring machine.	35
Figure 4-2 A. Plastic spatula and rubber bowl for mixing, B. Black plastic syringe (Sulzer®).	36
Figure 4-3 A. FTIR (PerkinElmer Series 2000, Beaconsfield, UK) and ATR accessory, B. Uncured adhesive was placed in a ring upon the ATR diamond and covered with acetate sheet, C. The light-cured from the top surface was set at 1 mm distance.	37
Figure 4-4 FTIR spectra upon polymerization obtained from the bottom of composites.	38
Figure 4-5 A. equipment for disc specimen preparation, B. LED 3rd generation: Demi Plus, Kerr, USA.	38
Figure 4-6 The prepared disc specimens (1 mm thickness x 10 mm internal diameter).	39
Figure 4-7 The schematic explaining the creation mass of m1 , m2 , and m3	40
Figure 4-8 A. computer-controlled universal testing machine (AGSX, Shimadzu, Kyoto, Japan), B. schematic of the ball-on-ring testing jig.	41
Figure 4-9 A. Disc specimen placed on ring support, B. Ball on ring test.	42
Figure 4-10 The process of sample preparation, A. the sample was positioned using wire and elastomeric ring upon a plastic sheet and supported by cylindrical PVC block, B. lateral view while preparing the sample, C. the prepared sample.	43
Figure 4-11 The sample was placed on a mechanical testing frame (AGSX, Shimadzu, Kyoto, Japan) for testing.	44
Figure 4-12 The schematic of ARI score.	45
Figure 4-13 Remaining adhesives on bracket base of samples in each group, which were taken from stereomicroscope.	45

Figure 4-14 A. Coating machine (Quoram Q150R ES®), B. SEM equipped with Energy Dispersive X-ray (EDX, Inca X-sight 6650 detector, Oxford Instruments, Abingdon, UK).....	46
Figure 5-1 Degree of monomer conversion of each experimental group. The lines indicate significant differences between groups ($p < 0.05$). Error bars are 95% CI ($n = 5$).....	49
Figure 5-2 The water sorption value of all experimental groups. The lines indicate significant differences between groups ($p < 0.05$). Error bars are 95% CI ($n = 6$).....	50
Figure 5-3 The water solubility value of all experimental groups. The lines indicate significant differences between groups ($p < 0.05$). Error bars are 95% CI ($n = 6$).....	51
Figure 5-4 Biaxial flexural strength (BFS) of all experimental groups at 24 h. The lines indicate significant differences between groups ($p < 0.05$). Error bars are 95% CI ($n = 7$).	52
Figure 5-5 Biaxial flexural modulus (BFM) of all experimental groups at 24 h. The lines indicate significant differences between groups ($p < 0.05$). Error bars are 95% CI ($n = 7$).	53
Figure 5-6 Boxplot exhibited enamel shear bond strength (SBS) of all experimental groups. The boxes represent the first quartile (Q1) to the third quartile (Q3), the horizontal lines in the box represent the median, the whiskers represent the maximum and minimum values ($n = 5$).....	54
Figure 5-7 The adhesive remnant area (%) of all experimental groups. The lines indicate significant differences between groups ($p < 0.05$). Error bars are 95% CI ($n = 5$).....	55
Figure 5-8 The percentage of the distribution of the ARI score of all experimental groups ($n = 5$).....	56
Figure 5-9 Bracket base of samples in each group, which were taken from stereomicroscope.....	56
Figure 5-10 SEM images of F1-Trans groups at magnification 1000 X. Red arrow pointed apatite-like crystals which only found in F1, F2, F3 and F4.	57
Figure 5-11 SEM images of F1(5000 X), F2(5000 X), F3(10000 X) and F4(10000 X) groups, exhibit apatite-like crystal configuration of each experimental group.....	57

Figure 5-12 EDX image of F3 found Calcium (Ca) and Phosphate (P).	58
Figure 5-13 Colony-forming unit of samples in each group, which were counted after 48 h of incubation at 37 °C 5 % CO ₂ atmosphere.	59
Figure 5-14 The mean of Log colony forming unit per millilitre (Log CFU/mL) of all experimental groups after 48 h of incubation at 37 °C 5 % CO ₂ atmosphere. The lines indicate significant differences between groups ($p < 0.05$). Error bars are 95% CI (n = 3).	60



List of Abbreviation

Symbols/Abbreviations	Terms
ACP	Amorphous calcium phosphates
Andro	Andrographolide
ARI	Acrylic remnant index
BAGs	Bioactive glasses
BGNPs	Bioactive glass nanoparticles
BHI	Brain–heart infusion
Bis-GMA	Bisphenol A diglycidyl methacrylate
CaP	Calcium phosphate
CFUs	Colony forming units
CHX	Chlorhexidine
CQ	Camphorquinone
DC	Degree of conversion
DCPA	Dicalcium phosphates
EPS	exopolysaccharides
F	Fluoride
HA	Hydroxyapatite
HEMA	2-hydroxyethyl methacrylate
HGF-1	Human gingival fibroblasts-1

MCPM	Monocalcium phosphate monohydrate
MMP	Matrix metalloproteinases
NACP	Nanocomposite containing amorphous calcium phosphate
NaF	Sodium fluoride
NAg	Silver nanoparticles
OH-	Hydroxyl group
QLF	Quantitative light-induced fluorescence
QoF	Quality of life
RI	Refractive indices
RMGIs	Resin-reinforced glass ionomer
SBF	Simulated body fluid
SBS	Shear bond strength
Si-ACP	Silica-modified amorphous calcium phosphate
SiOH	Silanol group
<i>S. mutans</i>	Streptococcus mutans
Sr-BAG	Strontium containing bioactive glass
SrBGNPs	Strontium-bioactive glass nanoparticles
Sr/CaP	Strontium / calcium phosphate which is strontium-bioactive glass nanoparticles (SrBGNPs) combine with monocalcium phosphate monohydrate (MCPM)

TCP	Tricalcium phosphate
β -TCP	β -tricalcium phosphate
TEGDMA	Triethylenegylcol dimethcarylate
TTCP	Tetracalcium phosphate
UDMA	Urethane dimethacrylate
WSL	White spot lesions
XRD	X-ray diffraction

Chapter 1 Introduction

Dental caries is the most common complication observed with orthodontic treatment by fixed orthodontic appliances associated with suboptimal oral hygiene (Tufekci et al., 2011; Mei et al., 2017). The orthodontic appliances hindered tooth cleaning, thereby promoting the retention of dental biofilm (Mei et al., 2017; Müller et al., 2021). Additionally, the dysbiosis of biofilm increased in the numbers of acid-tolerance and acid-producing bacterial such as *Streptococcus mutans* within the dysbiosis biofilm was observed (Shukla et al., 2017; Lucchese et al., 2018; Mummolo et al., 2020; Müller et al., 2021). Demineralization by acids leads to the loss of minerals results in the formation of incipient caries lesions which may appear as white spot lesions (WSL) in enamel. This lesion represents a significant challenge to achieve the excellent esthetic outcome (Sundararaj et al., 2015; Lopatiene et al., 2016).

It was reported that the incidence of white spot lesions (WSL) occurring during orthodontic treatment was between 30 % and 70 %. Maxillary anterior teeth and the areas around brackets were the most commonly affected sites (Heymann and Grauer, 2013; Sundararaj et al., 2015; Mei et al., 2017). Several interventions were proposed to inhibit the enamel demineralization in orthodontic treatments, such as the use of fluoride and non-fluoride products, chlorhexidine mouth rinse, diet modification (Höchli et al., 2016). The effectiveness of such interventions was mainly governed by unreliable patient compliance, especially for children and teenage patients (Heymann and Grauer, 2013). Therefore, the proposed alternative approach to prevent WSL was to develop orthodontic adhesives that exhibit remineralizing and antibacterial effects. This could potentially help to reduce the risk of caries formation around brackets.

Calcium phosphate (CaP) compounds are excellent ion-releasing fillers which could encourage the hydroxyapatite $[\text{Ca}_{10}(\text{PO}_4)_6(\text{OH})_2]$ that could subsequently promote tooth remineralization. The apatite is the final stable product in the precipitation of calcium and phosphate ions from neutral or basic solutions (pH of 7 – 9 at 37 °C) (Dorozhkin and Epple, 2002). Several bioactive composites have been developed which can promote the release of calcium and phosphate ions in the presence of an aqueous solution (Chiari et al., 2015; Alania et al., 2016; Aljabo et al., 2016). The released ions at the suitable pH enable the precipitation of calcium phosphate apatite (Xu et al., 2009). These bioactive

composites demonstrated remineralizing effects in the *in vitro* caries-like enamel lesions (Panpisut et al., 2016; Kangwankai et al., 2017). Monocalcium phosphate monohydrate (MCPM) is an excellent ion-releasing filler due to its highly hydrophilic characteristics. However, the addition of MCPM to resin composites negatively affected the polymerization and mechanical properties of the materials (Panpisut et al., 2016).

Bioactive glasses (BAGs) containing silicate or phosphate systems (SiO_2 , Na_2O , CaO , and P_2O_5) have been used in dentistry for enamel remineralization. The remineralization of enamel defects or WSL was enhanced by releasing of calcium and phosphate ions which precipitate to form hydroxyapatite (Bakry et al., 2014; Fernando et al., 2017). Substitution SrO of CaO in bioactive glass results in the expansion of the glass network, thereby enhancing ion releasing from the material (Fredholm et al., 2010; Fredholm et al., 2011). A study demonstrated Strontium-containing bioactive glass (Sr-BAG) exhibited antibacterial action (Liu et al., 2016). The use of nanoparticle bioactive glass as the ion-releasing filler also demonstrated the desirable remineralizing and antibacterial effects with the minimal effect on the mechanical properties of the materials (Nam et al., 2019).

Another attempt to enhance anti-caries effects for orthodontic adhesives was to enable antibacterial actions. Andrographolide (Andro) is a diterpenoid lactone extracted from the traditional medical herb *Andrographis paniculata*. Andrographolide exhibited a broad range of biological activities such as anti-inflammatory, antiviral, antitumor, antioxidant, and antibacterial properties (Limsong et al., 2004; Jiang et al., 2009; Wang et al., 2011; Arifullah et al., 2013; Banerjee et al., 2017). Andro inhibited the bacterial quorum-sensing system in the biofilm formation process of *Pseudomonas aeruginosa*, and inhibited the growth of gram-positive as *Staphylococcus aureus* (Jiang et al., 2009; Banerjee et al., 2017). Moreover, the extract from *Andrographis paniculata* could inhibit adherence of *Streptococcus mutans* to hydroxyapatite beads by decreased the activity of glucosyltransferase and also eliminated or decreased the activity of glucan-binding lectin from strains (Limsong et al., 2004).

The aim of this study was to prepare orthodontic adhesive containing strontium-bioactive glass nanoparticles (SrBGNPs) and monocalcium phosphate monohydrate (MCPM) as remineralizing agents. Andrographolide (Andro) was added as an antibacterial agent.

Different formulations of the experimental orthodontic adhesives containing a high and low level of Sr/CaP (SrBGNPs + MCPM) and Andro were prepared. The effect of increasing Sr/CaP and Andro levels on the degree of monomer conversion, water sorption and solubility, biaxial flexural strength / modulus, shear bond strength to enamel, ARI score, apatite formation ability, ion release, and the inhibition of *S. mutans* growth were assessed. The commercial orthodontic adhesive (Transbond XT, 3M) was used as the comparison.



Chapter 2 Review of literature

2.1 Orthodontic treatment

Malocclusion is defined as an irregularity of the teeth or a mal-relationship of the dental arches beyond the range of what is accepted as normal. It is the third-highest prevalence among oral pathologies, second only to tooth decay and periodontal disease (Tak et al., 2013). The reported prevalence of malocclusions is over 60 % in preschool children and between 43 and 78 % in schoolchildren (Dimberg et al., 2015). Although malocclusion is not a life-threatening event, it can cause psychological problems such as low self-esteem due to impaired dentofacial aesthetics (Tristão et al., 2020). It was reported that maxillary anterior crowding, excessive overjet with incomplete lip closure, and large diastema between incisors had been associated with the esthetic problem and lower self-esteem among teenagers (Dimberg et al., 2015; Tristão et al., 2020). Moreover, several studies revealed the impact of malocclusion on quality of life, such as speech and mastication problems (Silva et al., 2016; Abreu, 2018).

Because of the implications of malocclusion in the abovementioned, the demand for orthodontic treatment has been increased rapidly in Thailand (Chuacharoen, 2014). The levels of treatment need are usually governed by the socio-economic, ethnic differences, long treatment duration and facial appearance (Kazancı et al., 2016). The impaired dentofacial appearance was regarded as a decisive factor for patients seeking comprehensive orthodontic treatment (Chuacharoen, 2014; Taghavi Bayat et al., 2017).

2.2 Orthodontic adhesive

The orthodontic adhesive is essential for the fixation of brackets to teeth. The most commonly used orthodontic adhesives are resin composite orthodontic adhesive that requires enamel conditioning to enhance micro-mechanical interlocking (Gange, 2015). Enamel etching increases the adhesive properties of orthodontic adhesives on the prepared enamel surface, aiming to produce a strong micromechanical bond (Beltrami et al., 2016; Goldberg, 2016). The acid attacks the prism cores in enamel, leading to pores 5 - 6 μm in diameter, extending to a depth of 20 - 50 μm . The adhesive extends into the pores, forming an intimate irregular interface (Goldberg, 2016).

There are two main adhesive systems available. The first is conventional adhesive system which use 3 different agents (an acid solution, a primer solution, and an adhesive resin) in the process of bonding orthodontic brackets to the enamel. The second system is self-etch adhesive system which combine the acid and priming agents into a single acidic primer solution for simultaneous use on the enamel surface (Al Maaitah et al., 2013; Bucur et al., 2020). The studies demonstrated that the use of self-etch adhesive system to bond the orthodontic brackets to the enamel surface resulted in a significantly lower shear bond strength compared with the conventional adhesive system (Takamizawa et al., 2016; Zope et al., 2016; Bucur et al., 2020). However, a study illustrated that the self-adhesive system had less residual adhesive remaining on the tooth surface (ARI) compared with the conventional adhesive (Zope et al., 2016).

2.3 Enamel demineralization / white spot lesion (WSL) due to fixed orthodontic treatment

The dysbiosis biofilm produces an acidic environment causing dissolution of the underlying enamel (Klein et al., 2015; Paula et al., 2017). Enamel is an acellular hard tissue, which does not have the capacity to self-regenerate and leads to the loss of minerals (demineralization). Due to the significant difference of the refractive indices (RI) of the enamel demineralization area (RI = 1.3) compared with sound enamel (RI = 1.6), a whitish opaque appearance of these lesions can be observed (Figures 2-1,2). This phenomenon is called a white spot lesion (WSL) (Guerra et al., 2015). This may lead to uncleanable cavitated lesions or pulpal infection if the lesions are left untreated (Pinto et al., 2020).

It was proposed that the fixed orthodontic appliances may encourage the accumulation of biofilm. Furthermore, irregular shapes of the appliances may restrict the self-cleansing ability of saliva, lips, tongue, and cheeks. This may subsequently increase the risk of incipient caries on enamel surfaces (Chambers et al., 2013; Heymann and Grauer, 2013; Lopatiene et al., 2016; Müller et al., 2021).



Figure 2-1 Orthodontic white spot lesions (WSL) on enamel surfaces; these were adjacent to labial fixed orthodontic appliances (Chapman et al., 2010). Reprinted from *American Journal of Orthodontics and Dentofacial Orthopedics*, Vol 138-2, Chapman JA, Roberts WE, Eckert GJ, Kula KS, González-Cabezas C, *Risk factors for incidence and severity of white spot lesions during treatment with fixed orthodontic appliances*, Pages 188-194, Copyright (2010), with permission from Elsevier

The prevalence of WSL across the studies was inconsistent, which ranged from 39.6 % to 72.9 %. This may be due to the different protocols for detecting WSL in each study (Beerens et al., 2015; Lopatiene et al., 2016; Mei et al., 2017; Pinto et al., 2020). The common detectable site for WSL was at the junction between bonding agent and enamel surface at the peripheral of the bracket base (Chapman et al., 2010; Heymann and Grauer, 2013). Additionally, the most commonly affected tooth was lateral incisors followed by canines, premolars, and central incisors (Heymann and Grauer, 2013; Mei et al., 2017).



Figure 2-2 QLF images: the dark areas are areas of demineralization (Al Maaitah et al., 2011). Reprinted from *American Journal of Orthodontics and Dentofacial Orthopedics*, Vol 2, Al Maaitah EF, Adeyemi AA, Higham SM, Pender N, Harrison JE, *Factors affecting demineralization during orthodontic treatment: a posthoc analysis of RCT recruits*, Pages 181-191, Copyright (2011), with permission from Elsevier

2.4 The effect of the fixed orthodontic appliances on bacterial colonization

The placement of fixed orthodontic appliances on tooth surfaces created a greater surface area for bacterial attachment and promoted the growth of dental biofilm (Figure 2-3) (Chambers et al., 2013; Heymann and Grauer, 2013; Lopatiene et al., 2016; Müller et al., 2021). The critical site for dental plaque accumulation was the excess composite or adhesive around the bracket base (Heymann and Grauer, 2013). This may be due to its rough surface and the presence of a gap between the composite and enamel surface (Sukontapatipark et al., 2001). A study demonstrated that bacterial accumulation was not significantly different among different orthodontic adhesive materials such as Concise, Concise and Solo, Fuji LC, Sequence, Transbond (Badawi et al., 2003).

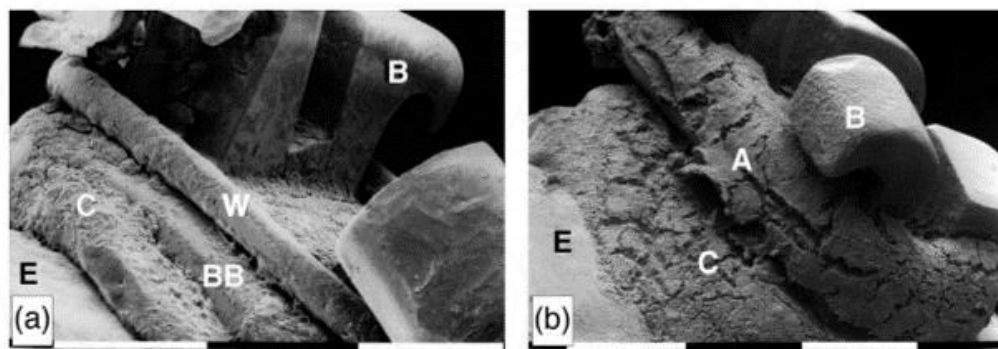


Figure 2-3 SEM images of plaque accumulation around the bracket. (a) Bonded tooth ligated with stainless steel wire (W) reveals abundant plaque deposition on excess composite, under bracket wings, and on and under the ligature wire, whereas sparse plaque is present on the enamel cervical to composite. The enamel-composite junction cannot be characterized due to the heavy plaque deposit. B, bracket wing; BB, bracket base; C, composite; E, enamel)(Sukontapatipark et al., 2001) Reprinted from Sukontapatipark W, El-Agroudi MA, Selliseth NJ, Thunold K, Selvig KA, *Bacterial colonization associated with fixed orthodontic appliances, The European Journal of Orthodontics*, 2001, vol 23(5), Pages 475-484, Copyright (2001) by permission of Oxford University Press

Streptococcus mutans (*S. mutans*) is the most commonly found bacteria in the cariogenic biofilm. Several studies demonstrated that the increase of *S. mutans* level in dental plaque in patients with fixed appliances was higher than in patients without fixed appliances (Heymann and Grauer, 2013; Mei et al., 2017; Lucchese et al., 2018; Mummolo et al., 2020). *S. mutans* is a major manufacturer of extracellular polymeric substances, including exopolysaccharides (EPS), the protein fibres, which could form a scaffold for the attachment of cells and other matrix components (Hobley et al., 2015; Klein et al., 2015).

It was proposed that EMS enhances microbial adherence on the tooth surface and also restrain biofilm diffusion. The EPS-rich matrix provides biofilm stability and facilitates the creation of highly acidic microenvironments, which are critical for the pathogenesis of dental caries (Klein et al., 2015).

2.5 The modification of orthodontic adhesive to reduce and prevent initial caries lesions (white spot lesions)

The prevention of enamel demineralization is an essential practice for orthodontists (Heymann and Grauer, 2013). The simplest way to prevent enamel demineralization is meticulous attention to maintain a high standard of oral hygiene. Most of the orthodontic patients, which were in the childhood and adolescent period, usually showed limited compliance of oral hygiene (Chambers et al., 2013; Tak et al., 2013). Therefore, several interventions were introduced to reduce the incidence of WSL (Derks et al., 2004; Kerbusch et al., 2012; Chambers et al., 2013). These adjunctive interventions may be achieved by the addition of remineralizing and antimicrobial agents.

2.5.1 Remineralizing agents

2.5.1.1 Fluoride

Fluoride (F) has been used to combat dental caries by reducing demineralization and enhancing remineralization of dental hard tissue. Fluoride ion is incorporated into the tooth structure and the hydroxyl group (OH⁻) of the hydroxyapatite. It results in the creation of a fluorohydroxyapatite lattice that is resistant to acid dissolution.

There are several fluoride-containing products for caries prevention, such as sodium fluoride (NaF) mouth rinses, NaF toothpaste, or fluoride varnish (Shinohara et al., 2009; Chambers et al., 2013; Yi et al., 2019). However, the effect of these adjunctive fluoride interventions is also governed by patient compliance (Chambers et al., 2013). Fluoridated bonding systems such as glass ionomer bonding material, resin-reinforced glass ionomer (RMGIs) cement and fluoride-containing adhesive were introduced (Shah et al., 2018; Benson et al., 2019; Bucur et al., 2020). A study showed that glass ionomer cement reduced demineralization around orthodontic brackets compared to bonding with composite resin during a 4-week period (Gorton and Featherstone, 2003). Additionally,

an *in vitro* study demonstrated RMGIs cement had higher F release than conventional glass ionomer cements and the highest release was at 24 hours (Dziuk et al., 2021). However, a clinical trial reported that the use of RMGIs cement failed to reduce the incidence of new WSL due to the limited level of fluoride release (Benson et al., 2019).

2.5.1.2 Monocalcium phosphate monohydrate (MCPM)

MCPM is the most acidic and water-soluble calcium phosphate compound (Dorozhkin and Epple, 2002). It is known that calcium and phosphate ions are essential for the formation of hydroxyapatite to promote remineralization of demineralized enamel. The previous studies demonstrated that the addition of MCPM promoted the formation of hydroxyapatite on the surface of resin composites (Figure 2-4) (Mehdawi et al., 2013; Aljabo et al., 2016). The composites in Figure 2-4 showed the increasing hydroxyapatite size due to elevated Ca, P content upon the immersion in body fluid. A study reported that composites containing mono/tricalcium phosphate combined with silica-silicon carbide nanoparticles resulted in a high concentration releasing of calcium and phosphate ions (Mehdawi et al., 2013).

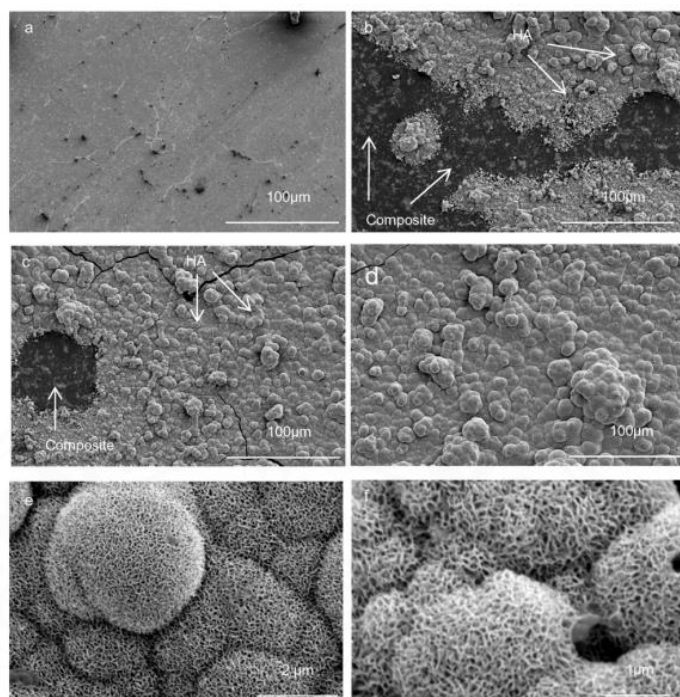


Figure 2-4 SEM images for composite (a) 0% CaP, (b) 10% CaP, (c, e and f) 20% CaP and (d) 40% CaP immersed in SBF for 1 week (Aljabo et al., 2016) Reprinted from *Materials Science and Engineering, Vol 60*, Aljabo A, Abou Neel EA, Knowles JC, Young AM, *Development of dental composites with reactive fillers that promote precipitation of antibacterial hydroxyapatite layers*, Pages 285-292, Copyright (2016), with permission from Elsevier

2.5.1.3 Strontium-bioactive glass nanoparticles (SrBGNPs)

Bioactive glasses (BAGs) are synthetic biomaterials that degrade in physiological fluid and release therapeutic ions, which form an apatite-like surface layer (Al-Eesa et al., 2017). It was first developed by Hench in 1969 for producing scaffolds devoted to bone regeneration due to their versatile properties (Kaur et al., 2014).

In dentistry, BAGs were first used for the management of dentin hypersensitivity by occluding exposed dentinal tubules with apatite formation using a calcium-sodium-phospho-silicate glass (Burwell et al., 2009). Several studies reported that BAGs might have the remineralizing effect, which is enhanced through the releasing of Ca and P ions (Brauer et al., 2010; Chatzistavrou et al., 2015; Al-Eesa et al., 2018). Furthermore, several studies demonstrated the antibacterial capacities of BAGs against many different bacterial

species *in vitro*, such as *S. mutans*, *A. actinomycetemcomitans*, and *P. gingivalis*, due to the pH elevation and changes in the osmotic pressure (Martins et al., 2011; Xu et al., 2015).

One approach to improving the properties of BAGs material is their development at the nanoscale (< 40 - 1000 nm). Reducing the size of BAGs granules facilitate the formation of the HA layer due to their small size and large active surface area, which promote BAGs solubility and ion release (Erol-Taygun et al., 2013; Carvalho et al., 2019). It had been reported that bioactive glass nanoparticles (BGNPs) have higher biocompatibility and also could stimulate their bioactivity (Ajita et al., 2015). Furthermore, BGNPs present a higher level of antibacterial effect as compared to the conventional BAGs, as a result of the capacity of the nanoparticles to release 10-fold more silica into simulated body fluid than conventional BAGs (Elkassas and Arafa, 2017). Additionally, a high level of released silica leads to the formation of silanol group (Si-OH), which act as the nucleation site for precipitation of calcium and phosphate ions determine the extent of remineralization (Elkassas and Arafa, 2017; Carvalho et al., 2019).

Strontium has an ionic radius of 1.16 Å, which was close to that of calcium (0.94 Å). The slight size difference allows the substitution of strontium for calcium in many crystal lattices. The substitution of a calcium ion by strontium ion in BAGs results in an expansion of the glass network. This was associated with the larger size of the Sr^{2+} compared to Ca^{2+} . The expansion of the glass network results in the weakening of the glass network (Fredholm et al., 2010; Fredholm et al., 2011). The expanded and weaken network significantly increased glass dissolution and ion release (Fredholm et al., 2011). Additionally, a study demonstrated that strontium containing bioactive glass (Sr-BAG) exhibited some antibacterial properties, which significantly inhibited the growth of *A. actinomycetemcomitans* and *P. gingivalis* (Liu et al., 2016).

2.5.2 Antibacterial agents

2.5.2.1 Chlorhexidine (CHX)

Chlorhexidine (CHX) is one of the most widely used antimicrobial agents, which possesses a broad spectrum of activity against oral bacteria. CHX was added into dental composites to enhance antimicrobial capacity (Mehdawi et al., 2013; Aljabo et al., 2016).

The CHX-containing composites showed a reduction of bacterial development compared to control samples that contained no CHX. However, the solubility of CHX was low; hence the high level of hydrophilic components was needed to promote the CHX release. This then subsequently reduced the mechanical properties of the composites (Mehdawi et al., 2013). The release of CHX may also cause brown staining that may affect the esthetic outcome (Van Strydonck et al., 2012). Moreover, acute and delayed reaction hypersensitivity resulted from using CHX products has been reported (Pemberton, 2016).

2.5.2.2 Silver nanoparticles (NAg)

The silver nanoparticles (NAg) are spherical nanoparticles with an average size of 30 ± 10 nm that are found to possess an excellent antibacterial effect at low concentrations (Baker et al., 2005; Park et al., 2013; Eslamian et al., 2020). The antibacterial properties were related to particle size, which smaller particles resulted in a greater surface area to volume ratio provided a more antibacterial efficiency (Baker et al., 2005; Elkassas and Arafa, 2017). The bactericidal mechanism of action was contributed from the penetration ability of NAg into the bacterial cell wall inducing peroxidation of the lipid component of the cell membrane result in membrane disruption (Park et al., 2013). In addition, the nanoparticles impede bacterial DNA replication lead to the incapability of bacterial cell repair (Liu et al., 2013; Elkassas and Arafa, 2017). Therefore, NAg was added into resin composite and the bonding agent to enable antibacterial capacity for the materials (Cheng et al., 2012; Cheng et al., 2016). Nevertheless, the incorporation of NAg may affect the colour and optical properties of the materials (Melo et al., 2013).

2.5.2.3 Andrographolide (Andro)

Andrographolide (Andro) is an active constituent extracted from *Andrographis paniculata* (Acanthaceae). The plant is generally recognized as King of bitters in English due to its bitter taste, Kalmegh in India, Hemptedu bumi in Malaysia, Fah Tah Lai Jone in Thailand, Chuan-Xin-Lin in China, and Senshinren in Japan (Low et al., 2015; Banerjee et al., 2017). Andro is a bicyclic diterpenoid containing γ -lactone in both ends of the molecule (Low et al., 2015). The chemical structure of Andro and related analogues are shown in Figure 2-5 (Jiang et al., 2009).

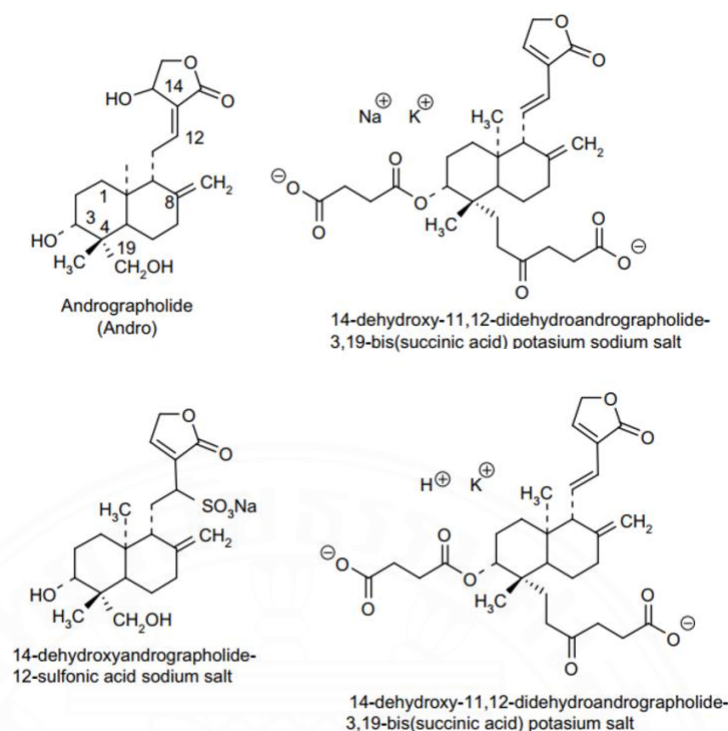


Figure 2-5 Chemical structure of Andrographolide (Andro) and related analogues (Jiang et al., 2009) Reprinted from *European journal of medicinal chemistry*, Vol 44(7), Jiang X, Yu P, Jiang J, Zhang Z, Wang Z, Yang Z, Tian Z, Wright SC, Larrick JW, Wang Y , *Synthesis and evaluation of antibacterial activities of andrographolide analogues*, Pages 2936-2943, Copyright (2009), with permission from Elsevier

Andro exhibited a wide range of biological activities such as anti-inflammatory, antiviral, antitumor, antioxidant, and antibacterial properties (Limsong et al., 2004; Jiang et al., 2009; Wang et al., 2011; Arifullah et al., 2013; Banerjee et al., 2017; Gupta et al., 2017; Mussard et al., 2019). In terms of antibacterial effect, several studies demonstrated the high effectiveness of Andro against several bacterial strains such as *Staphylococcus aureus*, *Streptococcus thermophilus*, *Bacillus subtilis*, *Escherichia coli*, *Mycobacterium smegmatis*, *Klebsiella pneumonia*, and *Pseudomonas aeruginosa* through different mechanisms (Li et al., 2006; Arifullah et al., 2013; Banerjee et al., 2017).

It was reported that Andro prevented biofilm colonization of *P. aeruginosa* by inhibiting the quorum-sensing system, which was essential for a cell-to-cell signaling mechanism (Li et al., 2006). Another study showed that Andro could prevent *S. aureus* biofilm formation by inhibiting intracellular DNA biosynthesis (Banerjee et al., 2017). A study demonstrated that the extract from *Andrographis Paniculata* could inhibit the adherence of *S. mutans* to hydroxyapatite beads by decreasing glucosyltransferase activity and

eliminating the activity of glucan-binding lectin from strains (Limsong et al., 2004). However, therapeutic use of andrographolide is limited due to its low water solubility (Gupta et al., 2017; Gaur et al., 2018; Mussard et al., 2019). In order to increase the water-soluble ability of Andro, the addition of hydroxypropyl- β -cyclodextrin (HP- β -CD) to Andro structure as guests in a cage-like meshwork was performed for enhancing solubility and dissolution rate (Ren et al., 2009).



Chapter 3 Statement of problems, objectives, and hypotheses

3.1 Statement of problems

It was proposed that the development of incipient dental caries (white spot lesions) around the dental brackets and orthodontic adhesives could be partially due to the lack of mineralizing and antibacterial actions of the current resin composite orthodontic adhesives. Therefore, the development of orthodontic adhesives that can promote ion release and antibacterial actions is needed. The addition of strontium-containing bioactive glass nanoparticles (SrBGNPs) with monocalcium phosphate monohydrate (MCPM) was expected to promote ion release. The addition of andrographolide (Andro) was expected to enhance antibacterial action for the experimental adhesives by the inhibition of *S. mutans* growth.

3.2 Objectives

1. The first objective was to prepare experimental orthodontic adhesives containing strontium-containing bioactive glass nanoparticles (SrBGNPs), monocalcium phosphate monohydrate (MCPM), and Andrographolide (Andro).
2. The second objective was to assess the effects of rising Sr/CaP (SrBGNPs + MCPM) level from 5 to 10 wt% and Andro from 5 to 10 wt% on the degree of monomer conversion, water sorption and solubility, biaxial flexural strength / modulus, shear bond strength to enamel, ARI score, mineral precipitation ability, ion release, and the inhibition of *S. mutans* growth of the experimental materials.
3. The third objective was to compare the degree monomer of conversion, water sorption and solubility, biaxial flexural strength / modulus, shear bond strength to enamel, ARI score, mineral precipitation ability, ion release, and the inhibition of *S. mutans* growth between the experimental adhesives and commercially available orthodontic adhesive.

3.3 Research hypotheses

1. It was hypothesized that the ion releasing and antibacterial resin composites orthodontic adhesive can be prepared.
2. The increase in Sr/CaP (SrBGNNPs + MCPM) levels from 5 to 10 wt% or the increase of Andro from 5 to 10 wt% should not significantly affect the degree of monomer conversion, water sorption and solubility, biaxial flexural strength / modulus, shear bond strength to enamel and ARI score, mineral precipitation ability, ion release, and the inhibition of *S. mutans* growth of the experimental adhesives.
3. The degree of monomer conversion, water sorption and solubility, biaxial flexural strength / modulus, shear bond strength to enamel and ARI score, mineral precipitation ability, ion release, and the inhibition of *S. mutans* growth of the experimental orthodontic adhesives should not be significantly different from those of the commercially available adhesive.

Chapter 4 Materials and methods

4.1 Materials preparation

All chemical used in the current study is shown in Table 4-1.

Table 4-1 Chemicals used in this study.

Abbreviation	Chemicals	Batch/lot number	Company
UDMA	Urethane dimethacrylate	MKCG8230	Sigma-Aldrich, MO, USA
TEGDMA	Tri-ethylene glycol dimethacrylate	STBF9549V	Sigma-Aldrich, MO, USA
HEMA	2-hydroxyethyl methacrylate	STBG9652	Sigma-Aldrich, MO, USA
CQ	Camphorquinone	09003AQV	Sigma-Aldrich, MO, USA
MCPM	Monocalcium phosphate monohydrate, particle diameter ~ 10 μm .	MCP-44950	Himed, NY, USA
SrBGnPs	Strontium-containing bioactive glass nanoparticles particle diameter ~ 200 nm.	-	Faculty of Engineering; King Mongkut's University of Technology North Bangkok (KMUTT)
Andro	Andrographolide (particle diameter ~ 10 – 50 μm)	NH20181005	Nanjing NutriHerb BioTech Co., Ltd
Glass 7 μm .	Silanated bariumaluminosilicate glass, particle diameter ~ 2 μm	806-128	Esstech Inc, IL, USA
Glass 0.7 μm .	Silanated bariumaluminosilicate glass, particle diameter ~ 0.7 μm	806-335	Esstech Inc, IL, USA

The liquid phase contained 70 wt% urethane dimethacrylate (UDMA) and 26 wt% triethylene glycol dimethacrylate (TEGDMA), 3 wt% 2-hydroxyethyl methacrylate (HEMA), and 1 wt% camphorquinone (CQ)(Table 4-2). The liquid was weighed using 4-figure balance (Mettler-Toledo GmbH, Im langacher 448606, Greifensee Switzerland), then was mixed by using a magnetic stirrer on a hotplate using 750 rpm for 30 mins (Figure 4-1).

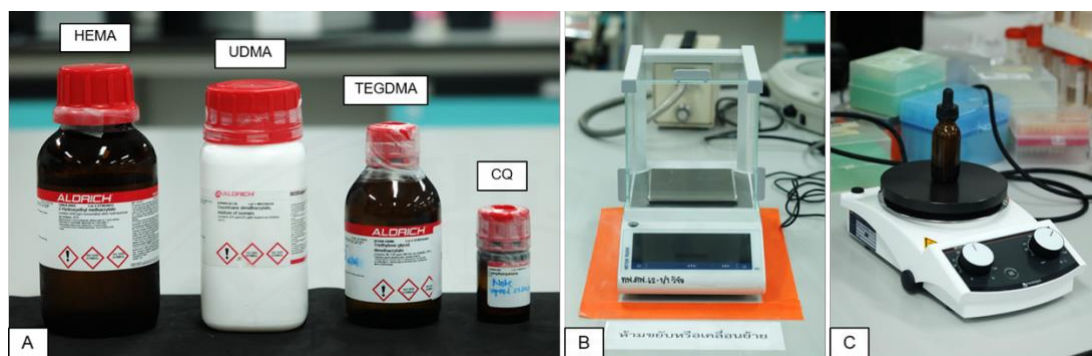


Figure 4-1 Chemical agents and tools for liquid phase preparation: A. liquid agents, B. The 4-figure balance, C. magnetic stirring machine.

Table 4-2 Formulation of the liquid component.

Liquid component	Chemicals	wt%
UDMA	Urethane dimethacrylate	70
TEGDMA	Tri-ethylene glycol dimethacrylate	26
HEMA	2-hydroxyethyl methacrylate	3
CQ	Camphorquinone	1

Five formulations of the experimental adhesives are provided in Table 4-3. The powder phase consisted of aluminosilicate glasses with a diameter of 0.7 μm and 7 μm . Strontium-containing bioactive glass nanoparticles combine with monocalcium phosphate monohydrate (Sr/CaP) for 0, 5, or 10 wt% was added for providing mineral precipitation effect. Additionally, andrographolide (Andro) for 0, 5, or 10 wt% was added for providing antibacterial capacities. The commercial adhesive (Transbond XT, Trans) was used as the commercial comparison (Table 4-4).

Table 4-3 The composition of the experimental orthodontic adhesives. The level of glass was reduced to maintain the total mass percentage of 100 wt%.

Component/formulations		F1	F2	F3	F4	F5
		(wt%)	(wt%)	(wt%)	(wt%)	(wt%)
Glass 7 μ m		40	42.5	42.5	45	50
Glass 0.7 μ m		40	42.5	42.5	45	50
Sr/CaP	SrBGNNPs	5	5	2.5	2.5	0
	MCPM	5	5	2.5	2.5	0
Andrographolide (Andro)		10	5	10	5	0
Total		100	100	100	100	100

Table 4-4 The information on ingredients of Tranbond XT light cure adhesive (3M Unitek, St. Paul, MN, USA as commercial control).

Ingredients	wt%
Silane treated quartz	70-80 Trade Secret*
Bisphenol A Diglycidyl Ether Dimethacrylate (Bis-GMA)	10-20 Trade Secret*
Bisphenol A Bis (2-Hydroxyethyl ether) Dimethacrylate	5-10 Trade secret*
Silane treated silica	<2 Trade Secret*
Diphenyliodonium Hexafluorophosphate	<1 trade Secret*

The experimental orthodontic adhesives were prepared with a powder to liquid ratio of 4:1. The powder and liquid phases were mixed using a spatula. The paste was kept in the non-light penetration syringe to prevent natural light induce polymerization (Figure 4-2).

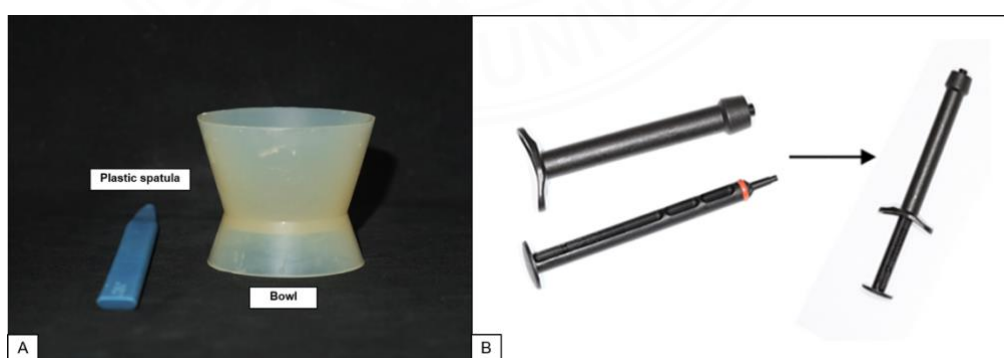


Figure 4-2 A. Plastic spatula and rubber bowl for mixing, B. Black plastic syringe (Sulzer®).

4.2 Degree of monomer conversion (DC)

The degree of monomer conversion of materials ($n = 5$) at room temperature (25 °C) was evaluated using FTIR (PerkinElmer Series 2000, Beaconsfield, UK) equipped with a golden gate Attenuated Total Reflectance (ATR) accessory. The uncured composite sample was placed in a circlip (1 mm thick and 10 mm diameter) over the ATR diamond and was covered with an acetate sheet. Then we recorded the initial absorbance and after light curing for 20 s of the C-O (1320 cm^{-1}). The materials were cured by an LED light-curing unit (1,100 - 1,330 mW/cm^2 , Demi Plus, Kerr, USA) at the top for 20 s (Figure 4-3). FTIR spectra in the area of 400 - 1700 cm^{-1} were recorded from the bottom of the sample. The degree of monomer conversion versus time was calculated using the following equation (Kangwankai et al., 2017).

$$C(\%) = \frac{100(\Delta A_0 - \Delta A_t)}{\Delta A_0} \quad \text{Equation 1}$$

ΔA_0 is the absorbance of the C-O peak (1320 cm^{-1}) initially before curing whilst ΔA_t is the absorbance of the C-O peak (1320 cm^{-1}) after 20 s of curing represent the C-O peak of the bottom surface of the composite samples. $C(\%)$ is percentage of curing unit.

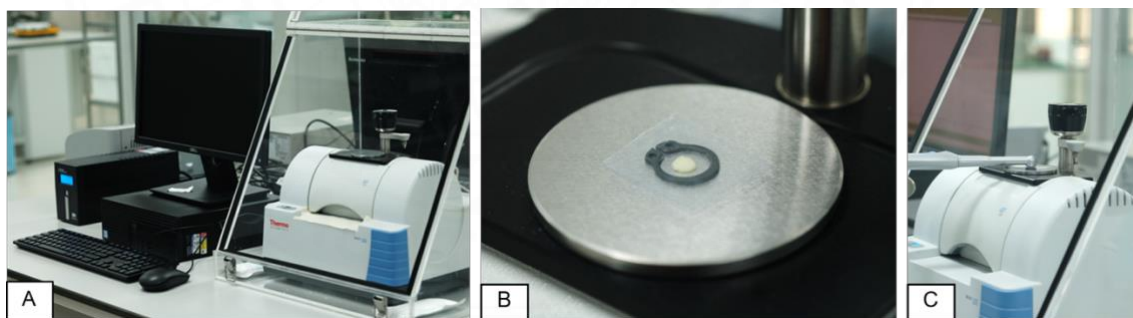


Figure 4-3 A. FTIR (PerkinElmer Series 2000, Beaconsfield, UK) and ATR accessory, B. Uncured adhesive was placed in a ring upon the ATR diamond and covered with acetate sheet, C. The light-cured from the top surface was set at 1 mm distance.

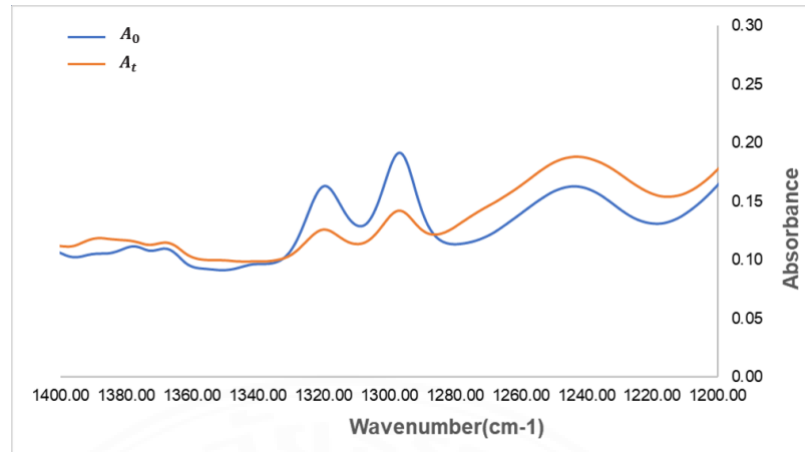


Figure 4-4 FTIR spectra upon polymerization obtained from the bottom of composites.

4.3 Water sorption (W_{sp}) and solubility (W_{sl})

Disc specimens (1 mm in thickness and 10 mm in internal diameter) were prepared using metal circlips as moulds ($n = 6$). The specimens were left at room temperature (25 °C) for at least 24 h to ensure completion of polymerization. After removal from the circlip, any excesses were trimmed. Specimens were stored in tubes containing 10 mL of deionized water at 37 °C until the required test time.

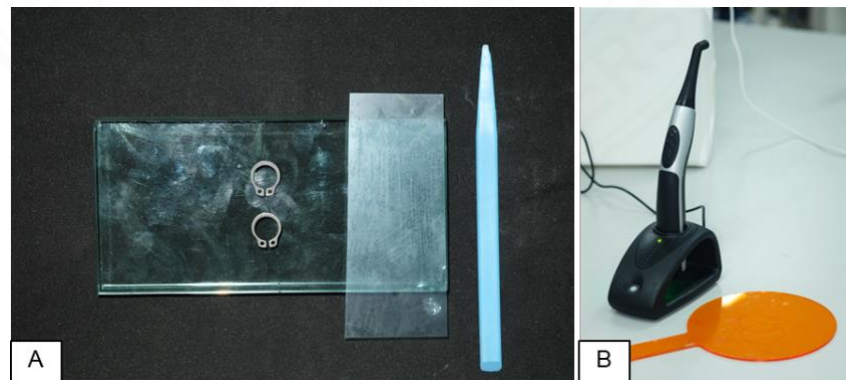


Figure 4-5 A. equipment for disc specimen preparation, B. LED 3rd generation: Demi Plus, Kerr, USA.

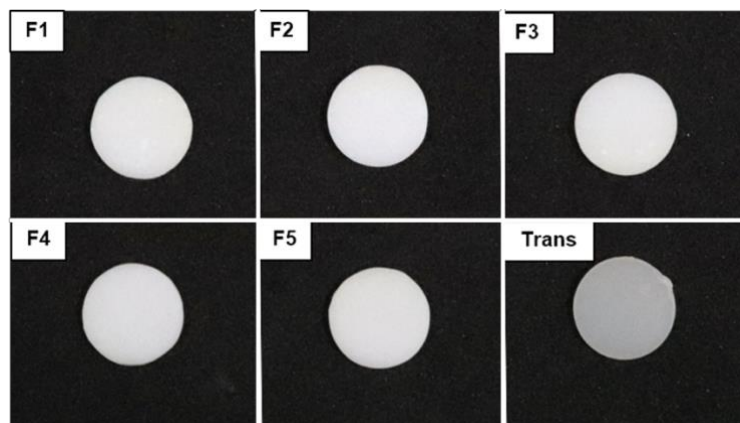


Figure 4-6 The prepared disc specimens (1 mm thickness x 10 mm internal diameter).

Water sorption and solubility were evaluated using a gravimetric study ($n = 6$). All prepared disc specimens were transferred into two desiccators which have different conditions (First desiccator 37 ± 2 °C for 22 h and second desiccator 23 ± 1 °C for 2 h). Disc specimens were transferred until the mass was constant as a conditioned mass which was an accuracy of 0.1 mg. Then, disc specimens were weighed using a 4-figure balance machine (m_1). After that, disc specimens were stored in 10 mL of deionized water at 37 °C. After 1, 2, 3, 4, 6, 24, 48 h and 1, 2, 3, 4, 5, 6 weeks, specimens were removed, blotted dry, reweighed (m_2) and replaced in new tubes containing fresh storage solution (Mehdawi et al., 2013). After reweighing of disc specimens (m_2), they were transferred into two desiccators again, then disc specimens were reweighed as a reconditioned mass (m_3).

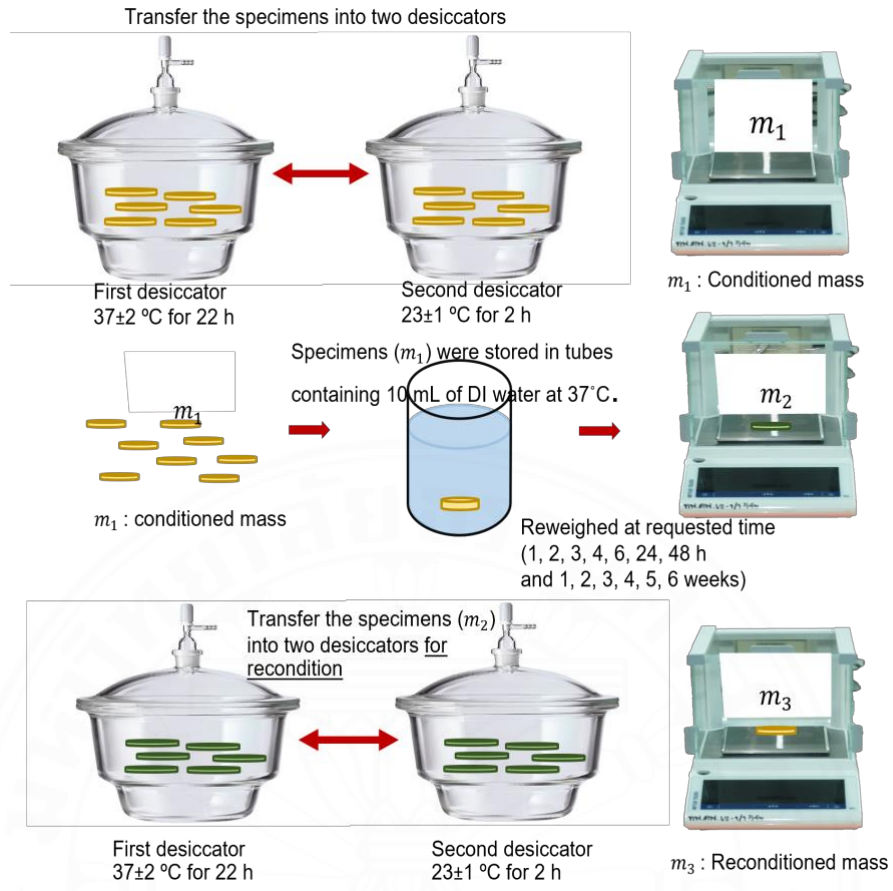


Figure 4-7 The schematic explaining the creation mass of m_1 , m_2 , and m_3 .

The water sorption (W_{sp}) and solubility (W_{sl}) values at each time point were calculated using the following equations.

$$W_{sp} = \frac{m_2 - m_3}{V} \quad \text{Equation 2}$$

$$W_{sl} = \frac{m_1 - m_3}{V} \quad \text{Equation 3}$$

W_{sp} and W_{sl} is the water sorption ($\mu\text{g}/\text{mm}^3$) and solubility values ($\mu\text{g}/\text{mm}^3$) whilst m_1 is the conditioned mass, in micrograms, prior to immersion in artificial saliva, m_2 is the mass of the specimen, in micrograms, after immersion in artificial saliva for requested time, and m_3 is the mass of the reconditioned specimen (μg). V is the volume of the specimen (mm^3).

4.4 Biaxial flexural strength (BFS) and biaxial flexural modulus (BFM)

Disc specimens ($n = 7$) were immersed in a tube containing 10 mL of deionized water and placed in an incubator at 37 °C for up to 4 weeks. A 500 N load cell was applied on a ball-on-ring testing jig with a spherical ball indenter (Figure 4-8). The crosshead speed of the test was set at 1 mm/min crosshead speed (AGSX, Shimadzu, Kyoto, Japan). The thickness of the specimen was recorded using a digital Vernier calliper.

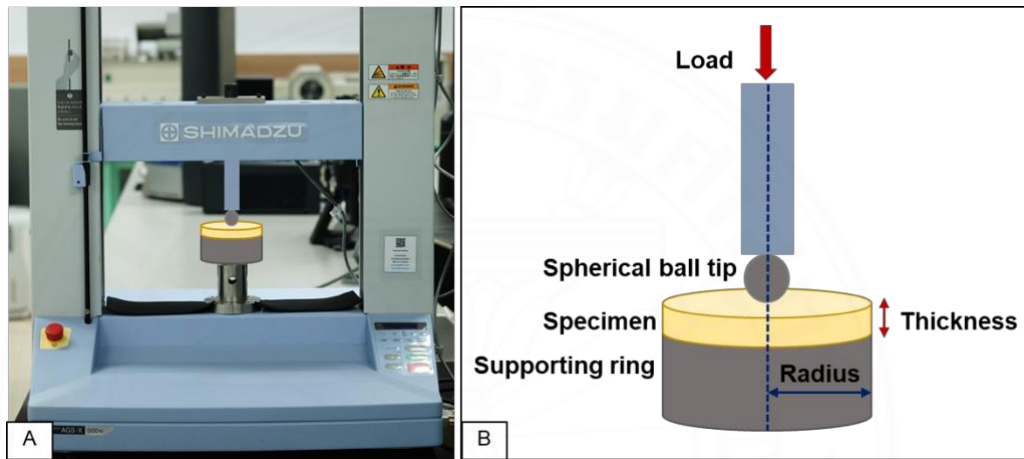


Figure 4-8 A. computer-controlled universal testing machine (AGSX, Shimadzu, Kyoto, Japan), B. schematic of the ball-on-ring testing jig.

The failure stress was recorded in newton (N), and the biaxial flexural strength (S; MPa) was calculated using the following equation 4.

$$S = \frac{F}{d^2} \left\{ (1 + \nu) \left[0.485 \ln \left(\frac{r}{d} \right) + 0.52 \right] + 0.48 \right\} \quad \text{Equation 4}$$

Where F is the load at failure (N), d is the specimen thickness (m), r is the radius of circular support (m), and ν is Poisson's ratio (0.3). Then, the biaxial modulus of elasticity was assessed by the following equation 5.

$$E = \left(\frac{\Delta H}{\Delta W_c} \right) \times \left(\frac{\beta_c d^2}{q^3} \right) \quad \text{Equation 5}$$

Where E is the modulus of elasticity of the specimen (GPa), $\frac{\Delta H}{\Delta W_c}$ is the rate of change of load with regards to central deflection or gradient of force versus displacement curve (N/m), β_c is centre deflection junction (0.5024), q is the ratio of support radius to the radius of the disc, and d is the specimen thickness (m) (Panpisut et al., 2016).

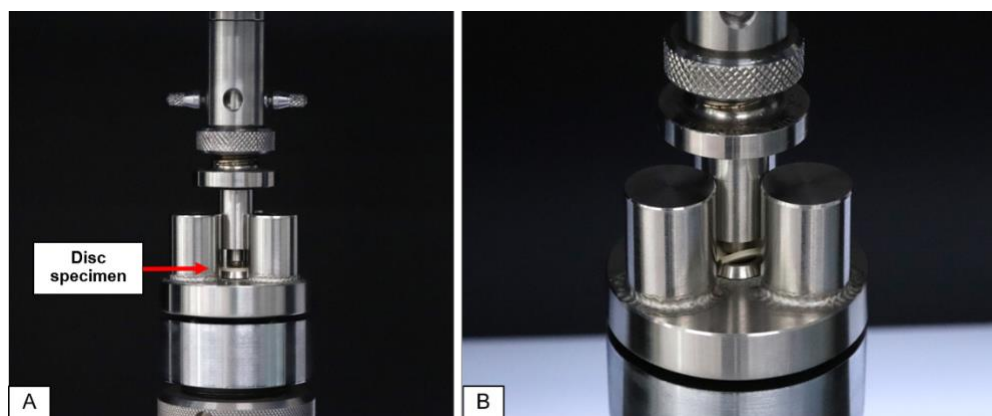


Figure 4-9 A. Disc specimen placed on ring support, B. Ball on ring test.

4.5 Shear bond strength (SBS) and adhesive remnant index (ARI)

The research ethic for collecting 30 human premolars was granted by The Ethical Review Sub-Committee Board for Human Research Involving Sciences, Thammasat University, No. 3 (Project No. 151/2563, 11 November 2020). The teeth were stored in 0.1 % thymol solution at 4 °C for less than 3 months. The teeth were examined under a microscope to detect any lesions on the buccal surface. The root of the tooth was cut with a diamond disc. The crown was cleaned using a prophylaxis cup and fluorine-free pumice, rinsed for 10 s and dried.

The buccal surface was etched using 35 % phosphoric acid (Transbond XT etching gel; 3M Unitek, Monrovia, CA, USA) for 15 s. The gel was rinsed for 15 s and dried. The primer (Transbond XT Light Cure Orthodontic Primer; 3M Unitek, Monrovia, CA, USA) was applied for 15 s and air-dried for 15 s. The adhesive was placed on a premolar bracket (GEMINI MBT 0.022 Twin; 3M Unitek) attached parallelly to the major axis of the tooth. The remaining paste was removed and light-cured at the mesial and distal sides at a distance of 2 mm for 40 s.

The tooth was embedded vertically into self-curing acrylic resin in a cylindrical PVC block. The buccal surface of the clinical crown was placed parallelly to the horizontal plane of the plastic sheet. The plastic sheet was used for compensating the bracket thickness. The tooth was positioned by using orthodontic rectangular wire and elastomeric ring to ensure that the buccal surface was parallel to the applied force in the shear bond strength test (Figure 4-10).

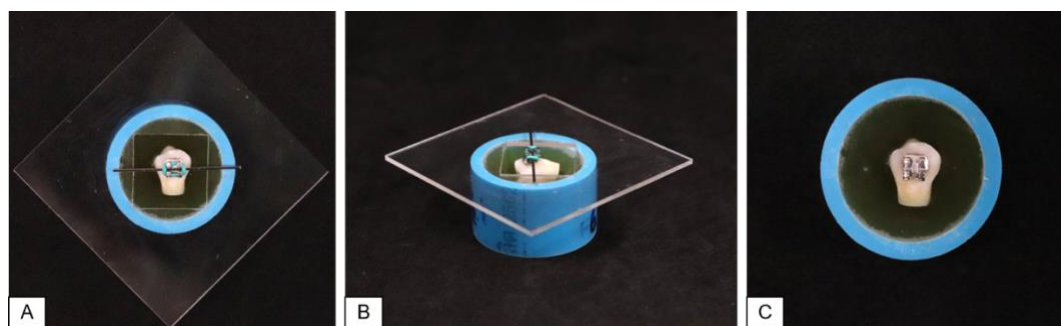


Figure 4-10 The process of sample preparation, A. the sample was positioned using wire and elastomeric ring upon a plastic sheet and supported by cylindrical PVC block, B. lateral view while preparing the sample, C. the prepared sample.

The SBS test was performed after the bracket-bonded samples were immersed in artificial saliva at 37 °C for 24 h. The chemical for preparing artificial saliva is provided in Table 4-5. The thermocycling process (Thermo Cycling, HWB332R, CWB332R, TC301) was performed between 5 °C and 55 °C for 500 cycles (30 s in each bath with a dwell time of 10 s).

Table 4-5 Composition of the artificial saliva (grams per litre).

Chemicals	Amount (g/L)
Methyl-p-hydroxybenzoate	2.00
Sodium Carboxymethyl Cellulose	10.00
KCL	0.625
MgCl ₂ •6H ₂ O	0.059
CaCl ₂	0.125
K ₂ HPO ₄	0.804
KH ₂ PO ₄	0.326

The pH of artificial saliva was adjusted to 6.75 with KOH.

Preparation of the artificial saliva

The bottle containing 1000 mL of distilled water was added with 2 g of methyl-p-hydroxybenzoate, 0.625 g of KCL, 0.059 g of MgCl₂•6H₂O, 0.125 g of CaCl₂, 0.804 of K₂HPO₄, and 0.326 of KH₂PO₄. All chemicals were weighed using a 4-figure balance. Then, the mixture was dissolved by using a magnetic stirrer on a hotplate using 750 rpm. Then, 10 g of sodium carboxymethyl cellulose was added and stirring until a total of

sodium carboxymethyl cellulose was dissolved. Then, the pH of artificial saliva was adjusted to 6.75 with KOH (Alshali et al., 2015).

The test was conducted using a shear bond strength testing jig under the computer-controlled universal testing machine (AGSX, Shimadzu, Kyoto, Japan)(Figure 4-11). The load in the occlusal-lingual direction was applied to the bracket base at a rate of 0.5 mm/min until the bracket was debonded. The SBS was calculated by dividing the load by the bracket contact surface area according to this equation 6 (Yi et al., 2019).

$$SBS = \frac{F}{A} \quad \text{Equation 6}$$

Where shear bond strength (SBS) was recorded in MPa, F is the force at bracket failure (Newtons), A is the surface area of the bracket (mm²) which was ~ 11.19 mm².

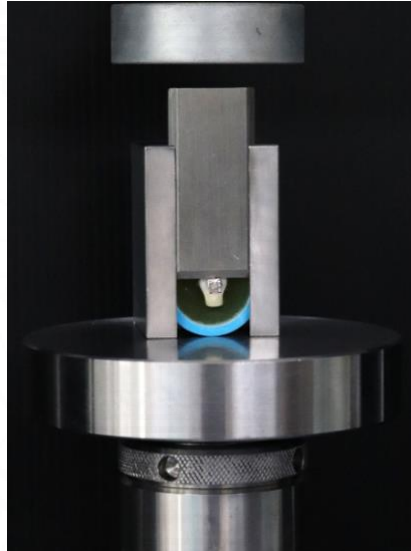


Figure 4-11 The sample was placed on a mechanical testing frame (AGSX, Shimadzu, Kyoto, Japan) for testing.

After brackets were detached, each brackets surface was observed under a stereomicroscope (Leica Zoom 2000, Leica Microsystems GmbH, Wetzlar, Germany) to examine the adhesive remnant index (ARI). The image from the stereomicroscope was calculated the area of remaining adhesive by ImageJ® software and inverted to truly remaining adhesive on enamel surface for ARI score. The ARI was determined by the remaining adhesive material on enamel, using the following criteria:(Melo et al., 2014)(Figure 4-12).

0 = no adhesive remained on enamel

- 1 = less than half of the adhesive remained on enamel
- 2 = more than half of the adhesive remained on enamel
- 3 = all the adhesive remained on enamel

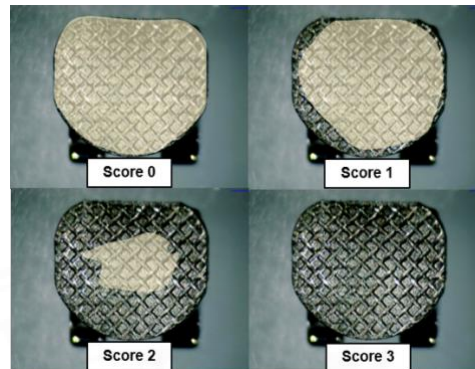


Figure 4-12 The schematic of ARI score.

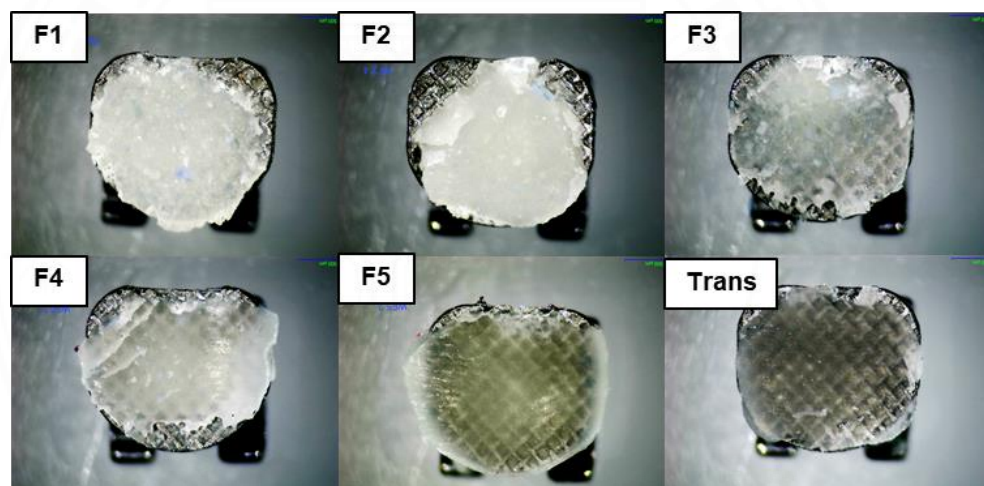


Figure 4-13 Remaining adhesives on bracket base of samples in each group, which were taken from stereomicroscope.

4.6 Mineral precipitation

The specimens were prepared according to section 4.5 were immersed in artificial saliva at 37 °C for 24 h. Then the specimens were debonded. The surface of the bracket base and enamel after debonding was sputtered with gold-palladium using a coating machine (Quoram Q150R ES®) and examined under a scanning electron microscope (SEM, JSM, 7800F, JEOL Ltd., Tokyo, Japan) to investigate the mineral precipitation. Additionally, Energy Dispersive X-ray Analysis (EDX, Oxford instrument) was employed to analyse the component or type of mineral precipitation (Kangwankai et al., 2017).

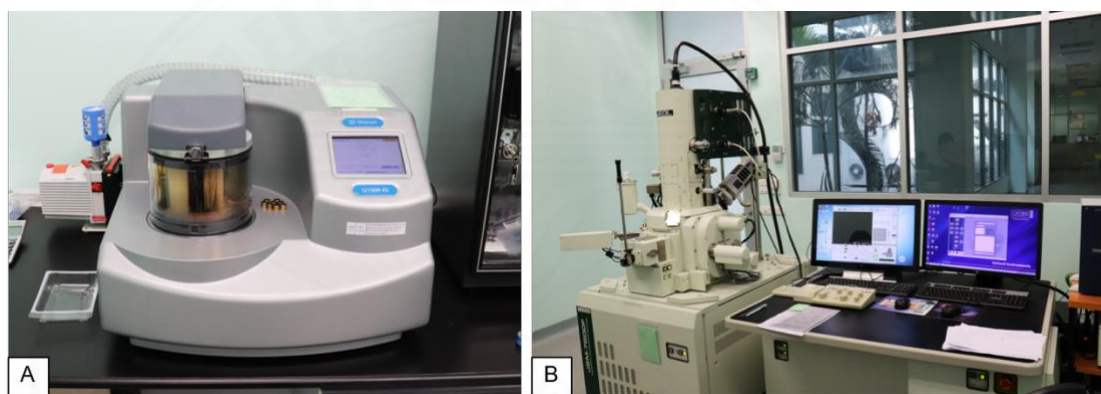


Figure 4-14 A. Coating machine (Quoram Q150R ES®), B. SEM equipped with Energy Dispersive X-ray (EDX, Inca X-sight 6650 detector, Oxford Instruments, Abingdon, UK).

4.7 Ion release

The storage solution from the water sorption / solubility tests was collected for assessing the ions concentration ($n = 3$). The collected solution was mixed with 3 vol% nitric acid. The standard calibration was performed using the instrument calibration standards. The ion concentration of Ca, P, Na, Al and Sr in the mixed solution was examined using the inductively coupled plasma atomic emission spectroscopy (ICP-OES, Optima 8300, PerkinElmer, Waltham, Massachusetts, USA). The result was analyzed using Syngistix™ for ICP software V.2.0 (PerkinElmer).

4.8 The inhibition of *S. mutans* growth

S. mutans (ATCC 25175) was cultured with Mueller Hinton broth (BD Difco™ Mueller Hinton Broth). The *S. mutans* suspension to Mueller Hinton broth ratio was 1:2 and incubated for 24 h at 37 °C 5 % CO₂ atmosphere. A suspension of *S. mutans* after growth was adjusted amount of cell growth by spectrophotometry at 600 nm optical density (OD). A suspension was adjusted to 0.5 MacFarland standard correspond to 2.5×10^8 cell/mL, then was serial diluted until 2.5×10^5 cell/mL as an initial concentration in this study.

Disc specimens with 10 mm diameter and 1 mm thickness were prepared (n = 3). The specimens were sterilized with UV irradiation (wavelength ~ 280 nm) for 30 min on both sides. The specimens were then immersed in the tube containing the mixture between 2 mL of Mueller Hinton broth and 1 mL suspension of *S. mutans* (2.5×10^5 cell/mL). The tubes were incubated for 48 h at 37 °C under the 5 % CO₂ atmosphere. Then, the discs were removed, the suspension was vortexed for 30 s, and serial diluted until 10^{-7} of cell/mL was obtained. Then, 200 µL of the suspension was pipetted and plated on Mitis Salivarius agar. The plates were then incubated for 48 h at 37 °C under the 5 % CO₂ atmosphere. The numbers of colony-forming units (CFUs) were counted under the microscope and image analysis. The results were presented as log CFU/mL values (Ferreira et al., 2019).

4.9 Statistical analysis

Data were analyzed using SPSS version V20.0 (IBM, Chicago, IL, USA) for Window. The Kolmogorov–Smirnov test and Levene test were performed to assess the normality and variances between groups. Data were analyzed using one-way analyses of variance (ANOVA) followed by post hoc Tukey's honestly significant difference test if the data is normally distributed and their variances are equal. If the variances were unequal, the result was tested with the Welch test followed by multiple comparisons using Dunnett's T3 test. Alternatively, the Kruskal-Wallis test was tested and followed by Dunn multiple comparisons if the data is not normally distributed. For ARI results, the Chi-square test was used to evaluate the scores among the experimental adhesive groups. Statistical significance was set at $p = 0.05$. Additionally, the effect of rising Sr/CaP and Andro levels from 5 wt% to 10 wt% on the tested properties was examined using factorial analysis,

which was used to quantify the effect from two variables (Sr/CaP, Andro) at two levels (5 or 10 wt%) used in the previously published studies (Panpisut et al., 2016; Panpisut et al., 2019)

Power of statistic was performed using G*Power 3.1 Software (University of Dusseldorf, Germany) based on previous studies (Melo et al., 2014; Panpisut et al., 2016; Kangwankai et al., 2017; Ferreira et al., 2019; Panpisut et al., 2019; Yi et al., 2019) and pilot study. Sample size in each test gave power > 0.95 at alpha = 0.05



Chapter 5 Results

5.1 Degree of monomer conversion (DC)

F5 exhibited the highest monomer conversion ($61.5 \pm 0.8 \%$), whereas Trans exhibited the lowest monomer conversion ($37.9 \pm 0.8 \%$). The conversion of F1, F2, F3 and F4 were $46.9 \pm 1.9 \%$, $46.8 \pm 6.4 \%$, $48.0 \pm 2.2 \%$, $45.9 \pm 2.6 \%$ respectively. The conversion of F5 was significantly higher than Trans ($p < 0.01$)(Figure 5-1). The monomer conversion of F1 was comparable to that of F2, F3 and F4 ($p > 0.05$). Factorial analysis indicated that the increase of Sr/CaP and Andro levels showed a negligible effect on monomer conversion.

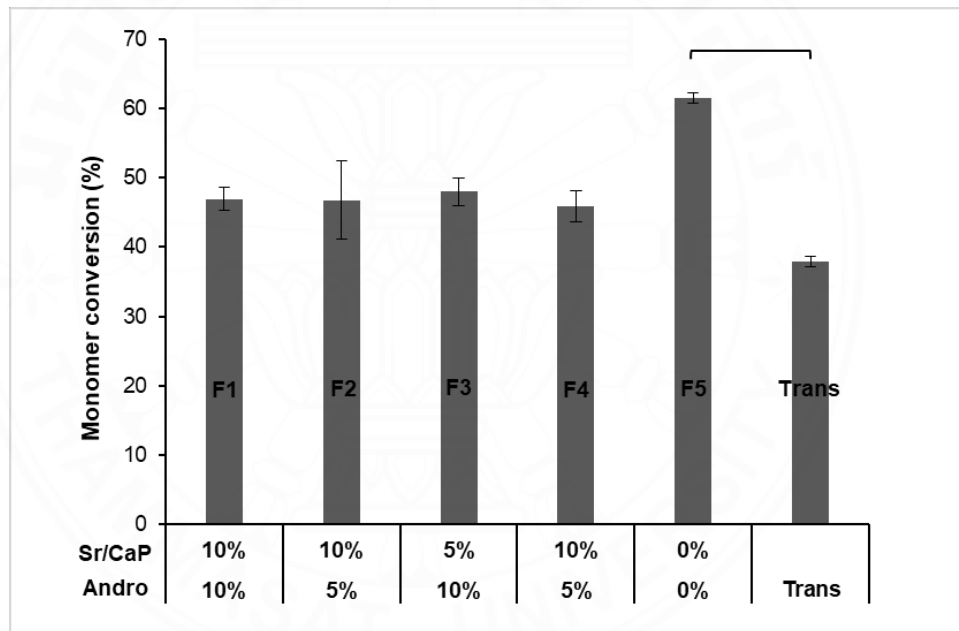


Figure 5-1 Degree of monomer conversion of each experimental group. The lines indicate significant differences between groups ($p < 0.05$). Error bars are 95% CI ($n = 5$).

5.2 Water sorption (W_{sp}) and solubility (W_{sl})

The highest and lowest water sorption were obtained from F2 ($48.6 \pm 1.5 \mu\text{g}/\text{mm}^3$) and Trans ($12.0 \pm 1.0 \mu\text{g}/\text{mm}^3$). The water sorption of F1, F3, F4 and F5 were $46.0 \pm 0.9 \mu\text{g}/\text{mm}^3$, $35.2 \pm 1.0 \mu\text{g}/\text{mm}^3$, $32.9 \pm 1.4 \mu\text{g}/\text{mm}^3$, $22.7 \pm 1.4 \mu\text{g}/\text{mm}^3$, respectively (Figure 5-2). The water sorption of F1 and F2 were significantly higher than that of F5 ($p < 0.05$) and Trans ($p < 0.01$). The water sorption of F1 was comparable to that of F2 ($p > 0.05$). The water sorption of F3 was similar to that of F4 ($p > 0.05$)(Figure 5-2). Factorial analysis indicated that the increase of Sr/CaP from 5 to 10 wt% increased water sorption by $39 \pm 4 \%$.

The highest and lowest water solubility were obtained from F1 ($5.9 \pm 1.3 \mu\text{g}/\text{mm}^3$) and F5 ($0.2 \pm 1.2 \mu\text{g}/\text{mm}^3$), respectively. The water solubility of F2, F3, F4 and Trans were $5.1 \pm 1.6 \mu\text{g}/\text{mm}^3$, $5.9 \pm 1.9 \mu\text{g}/\text{mm}^3$, $3.0 \pm 1.0 \mu\text{g}/\text{mm}^3$, $0.4 \pm 1.0 \mu\text{g}/\text{mm}^3$, respectively (Figure 5-3). F1, F2 and F3 showed significantly higher water solubility than F5 ($p < 0.05$). F1 and F3 also showed significantly higher water solubility than Trans ($p < 0.05$). The factorial analysis indicated that the increase of Andro from 5 to 10 wt% increase water solubility by $55.97 \pm 55.91 \%$.

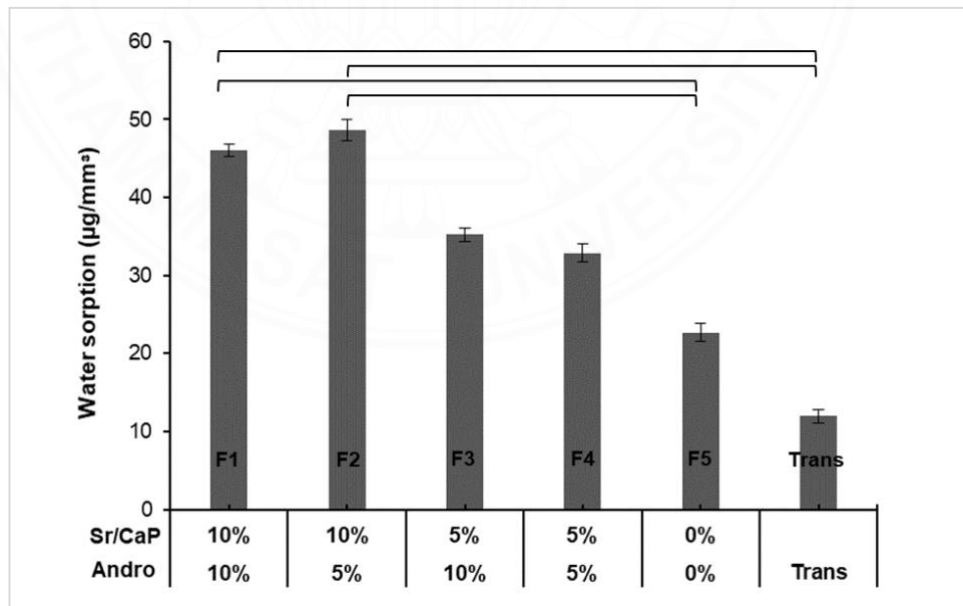


Figure 5-2 The water sorption value of all experimental groups. The lines indicate significant differences between groups ($p < 0.05$). Error bars are 95% CI ($n = 6$).

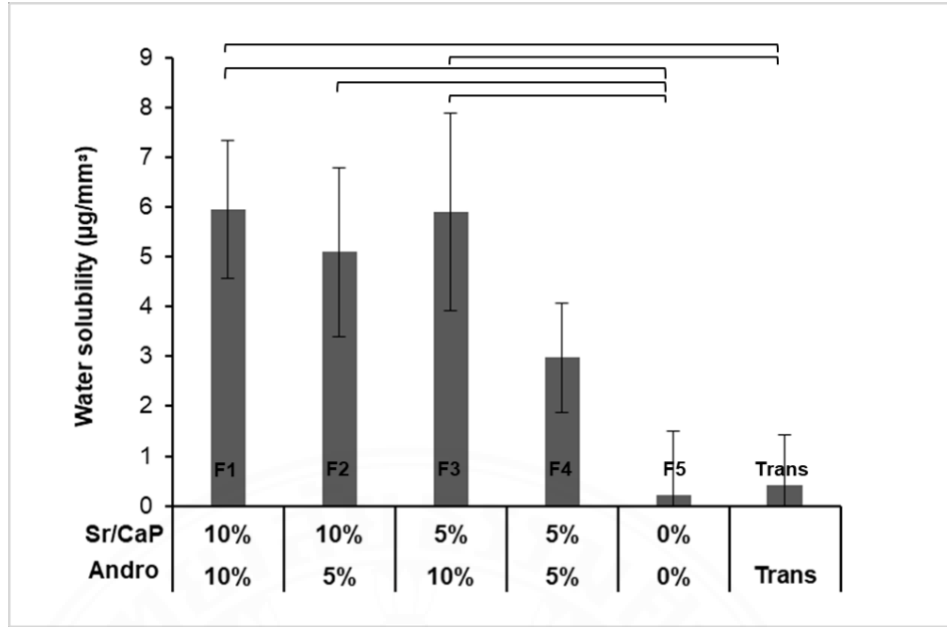


Figure 5-3 The water solubility value of all experimental groups. The lines indicate significant differences between groups ($p < 0.05$). Error bars are 95% CI ($n = 6$).

5.3 Biaxial flexural strength (BFS) and Biaxial flexural modulus (BFM)

5.3.1 Biaxial flexural strength (BFS)

The highest and lowest BFS were obtained from Trans (199 ± 22 MPa) and F1 (119 ± 6 MPa). The BFS of F2, F3, F4 and F5 were 143 ± 5 MPa, 122 ± 8 MPa, 147 ± 8 MPa, 193 ± 14 MPa, respectively (Figure 5-4). The BFS of F1 and F3 were significantly lower than that of F5 ($p < 0.01$) and Trans ($p < 0.01$). The BFS of Trans was comparable to that of F2 ($p = 0.207$), F4 ($p = 0.547$), and F5 ($p > 0.05$). Factorial analysis indicated that the increase of Andro from 5 wt% to 10 wt% reduced the BFS by 17 ± 4 %. However, the increase in the level of Sr/CaP showed a negligible effect on the BFS of the experimental materials.

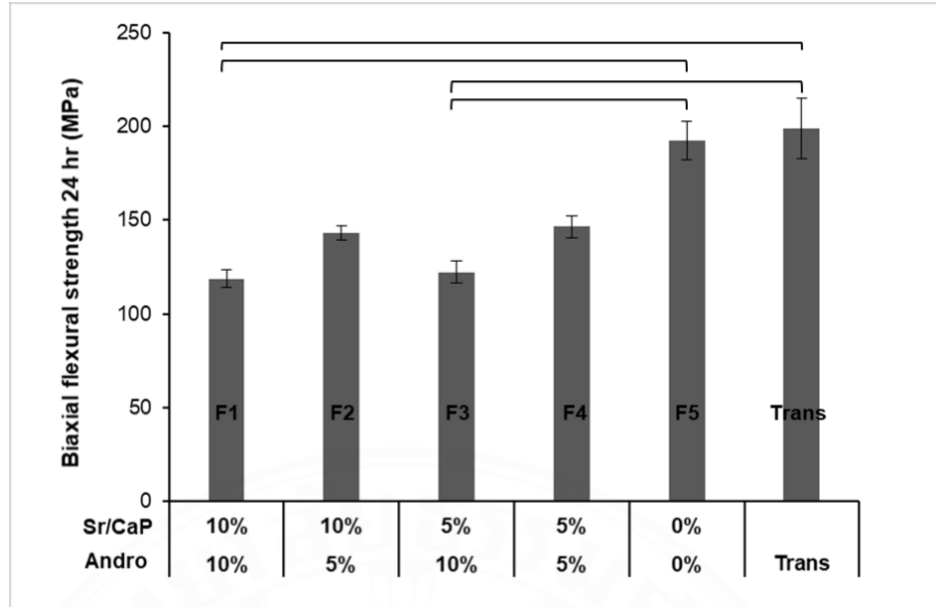


Figure 5-4 Biaxial flexural strength (BFS) of all experimental groups at 24 h. The lines indicate significant differences between groups ($p < 0.05$). Error bars are 95% CI ($n = 7$).

5.3.2 Biaxial flexural modulus (BFM)

The highest and lowest BFM were obtained from F5 (6.1 ± 0.5 GPa) and F1 (4.9 ± 0.2 GPa). The BFM of F2, F3, F4 and Trans were 5.3 ± 0.5 GPa, 5.0 ± 0.2 GPa, 5.4 ± 0.3 GPa, 5.7 ± 0.3 GPa, respectively (Figure 5-5). The BFM of Trans was comparable to that of F2 ($p = 0.461$), F4 ($p = 0.541$), and F5 ($p = 0.716$). F1 and F3 were significantly lower than that of F5 ($p < 0.05$) and Trans ($p < 0.01$). Factorial analysis showed that the increase of Andro from 5 wt% to 10 wt% reduced BFM by 10 ± 8 %. However, the increase of Sr/CaP showed a negligible effect.

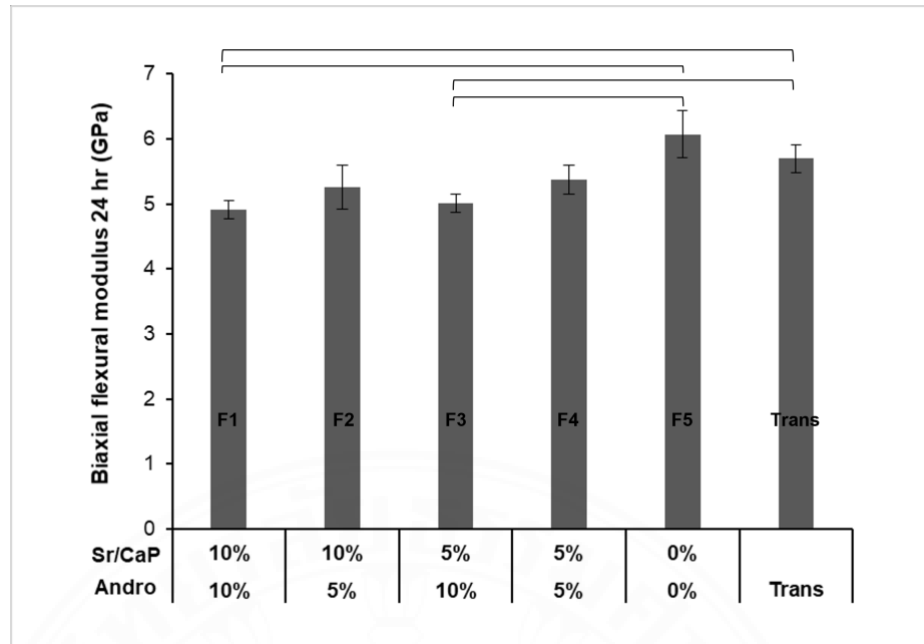


Figure 5-5 Biaxial flexural modulus (BFM) of all experimental groups at 24 h. The lines indicate significant differences between groups ($p < 0.05$). Error bars are 95% CI ($n = 7$).

5.4 Enamel shear bond strength (SBS) and adhesive remnant index (ARI)

5.4.1 Enamel shear bond strength (SBS)

The highest and lowest median of SBS were obtained from F5 (35, 25 - 42 MPa) and F2 (17, 14 - 30 MPa). The SBS of F1, F3, F4 and Trans were 18, 11 - 27 MPa; 26, 22 - 34 MPa; 27, 20 - 35 MPa; 27, 23 - 41 MPa, respectively (Figure 5-6). The SBS of Trans was comparable to that of F1, F2, F3, F4, F5 ($p > 0.05$). The factorial analysis demonstrated that the increase of Sr/CaP from 5 to 10 wt% reduced SBS by 28 ± 22 %. The effect from Andro was negligible.

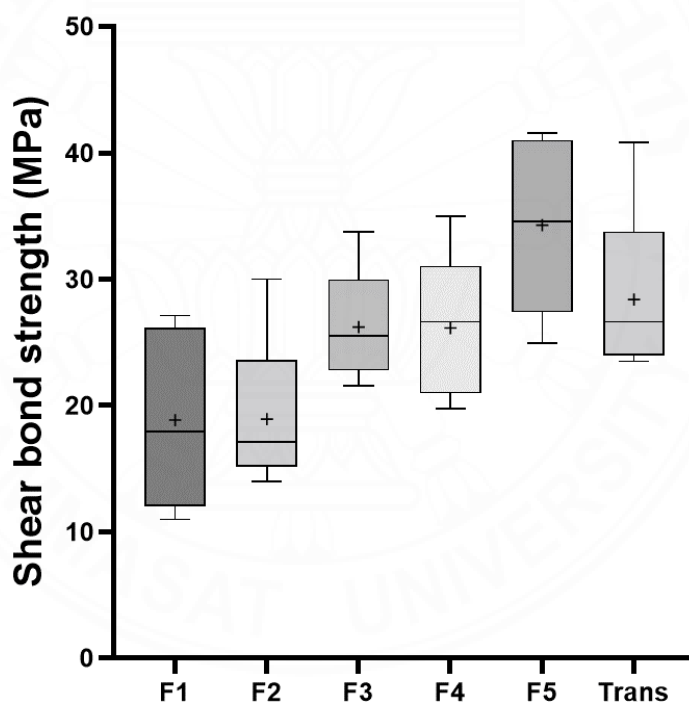


Figure 5-6 Boxplot exhibited enamel shear bond strength (SBS) of all experimental groups. The boxes represent the first quartile (Q1) to the third quartile (Q3), the horizontal lines in the box represent the median, the whiskers represent the maximum and minimum values ($n = 5$).

5.4.2 Adhesive remnant index (ARI)

The highest and lowest area of the adhesive remnant on enamel surface after dedonded were obtained from F2 (12.4 ± 12.2 %) and F5 (0 %). The adhesive remnant area (ARA) of F1, F3, F4 and Trans were 8.4 ± 3.2 %, 8.7 ± 3.2 %, 6.1 ± 6.2 %, 2.6 ± 3.1 %, respectively (Figure 5-7). F2 was significantly higher than F5 ($p = 0.035$). The adhesive remnant area of of Trans was comparable to that of F1 ($p = 0.660$), F2 ($p = 0.144$), F3 ($p = 0.611$), F4 ($p = 0.940$), and F5 ($p = 0.982$). Factorial analysis indicated that the increase of Sr/CaP and Andro from 5 wt% to 10 wt%, showed a negligible effect on the adhesive remnant area on enamel surface.

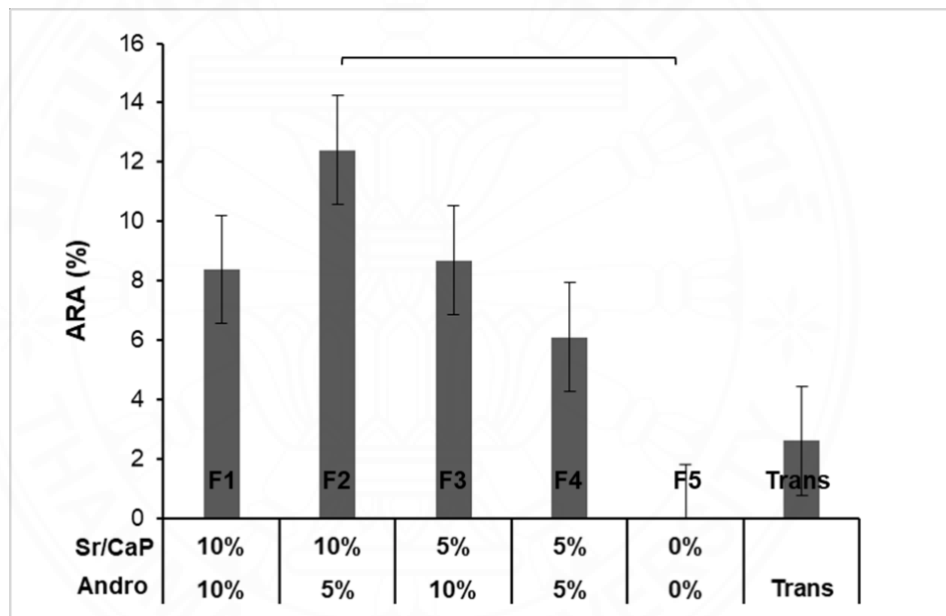


Figure 5-7 The adhesive remnant area (%) of all experimental groups. The lines indicate significant differences between groups ($p < 0.05$). Error bars are 95% CI ($n = 5$).

The percentage of the distribution of the ARI score obtained from each material is presented in Figure 5-8. The most common score observed from all materials were 0 and 1. The distribution of the score among each group was not significantly different ($p > 0.05$).

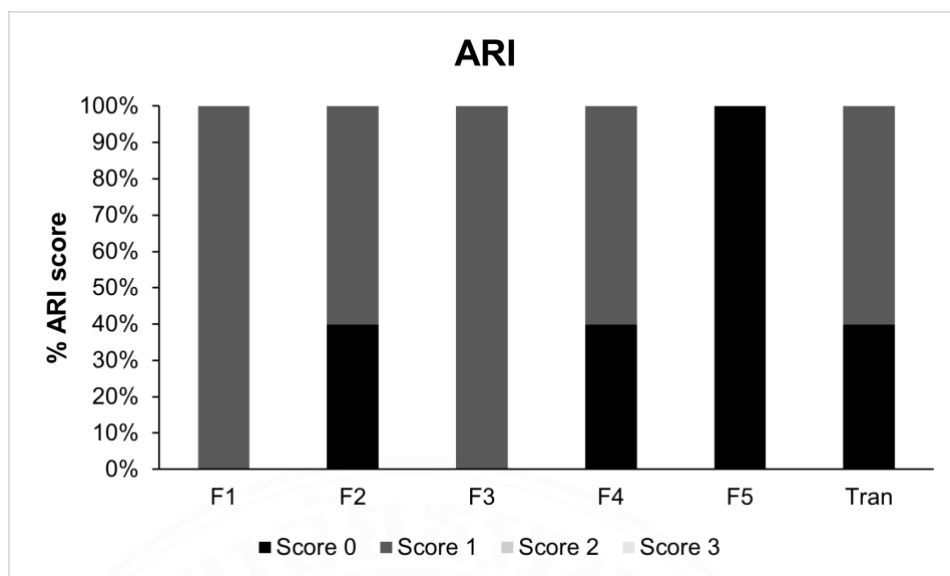


Figure 5-8 The percentage of the distribution of the ARI score of all experimental groups (n = 5).

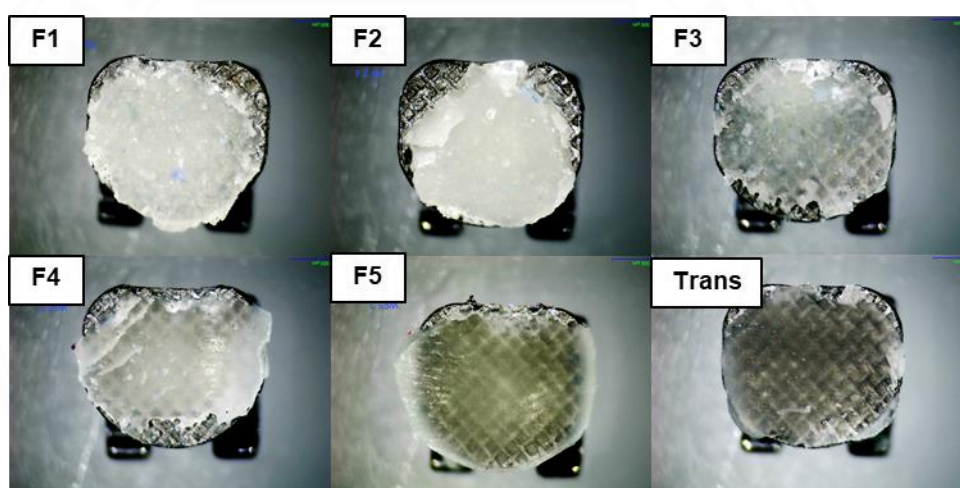


Figure 5-9 Bracket base of samples in each group, which were taken from stereomicroscope.

5.5 Mineral precipitation

The fracture surface of the debonded specimen demonstrated the precipitation of calcium phosphate crystals on the surface. The precipitation was not detected with F5 and Trans (Figures 5-10,11). The formation of calcium phosphate crystals was detected in F1, F2, F3, and F4. EDX result demonstrated that the precipitate contained Ca and P (Figure 5-12).

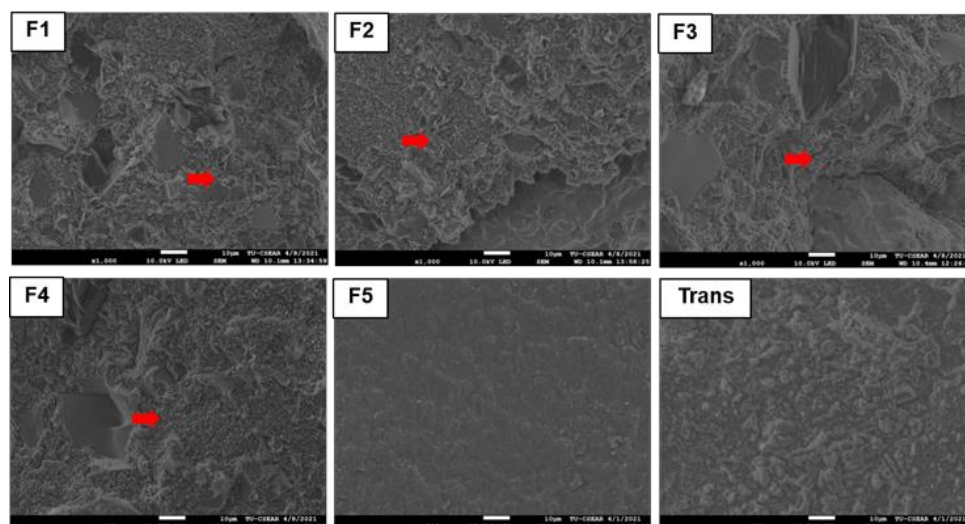


Figure 5-10 SEM images of F1-Trans groups at magnification 1000 X. Red arrow pointed apatite-like crystals which only found in F1, F2, F3 and F4.

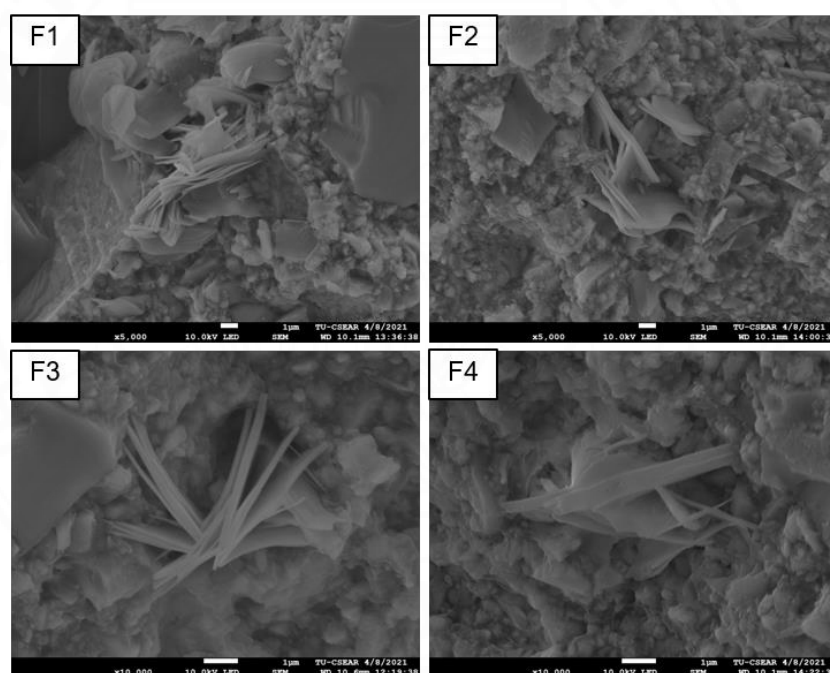


Figure 5-11 SEM images of F1(5000 X), F2(5000 X), F3(10000 X) and F4(10000 X) groups, exhibit apatite-like crystal configuration of each experimental group.

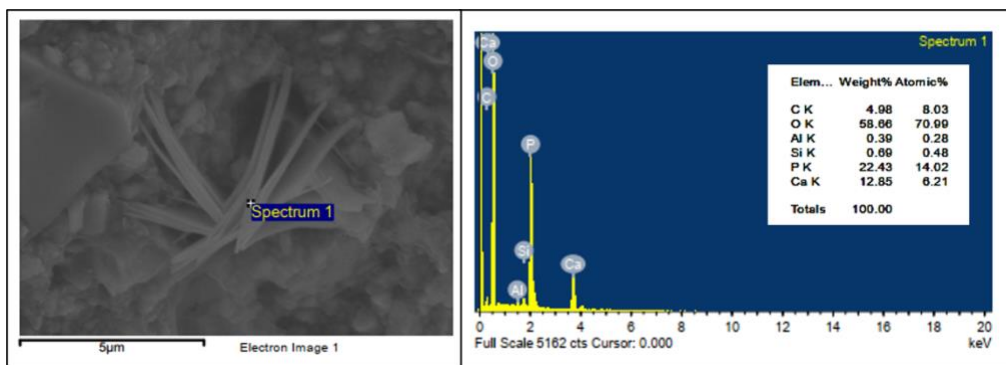


Figure 5-12 EDX image of F3 found Calcium (Ca) and Phosphate (P).

5.6 Ion release

Ca, P, and Sr ions were not detected with F5 and Trans (Table 5-1). The highest and lowest Ca ion release was detected with F2 (1.70 ± 0.29 ppm) and F4 (0.61 ± 0.02 ppm). For P ions, the highest and lowest concentration were detected with F2 (3.44 ± 0.10 ppm) and F4 (1.22 ± 0.03 ppm). Likewise, the highest and lowest Sr ions were detected with F2 (1.99 ± 0.73 ppm) and F4 (0.85 ± 0.22 ppm). The factorial analysis demonstrated that the increase of Sr/CaP from 5 to 10 wt% increased the released Ca and P ions by 141 ± 19 % and 119 ± 4 %, respectively. The effect from the increasing level of Andro was negligible. Sr/CaP and Andro levels showed a negligible effect on the released Sr ions of the experimental materials.

Table 5-1 Raw data of Ion release

	F1	F2	F3	F4	F5	Trans
Sr/CaP	10%		5%		0%	-
Andro	10%	5%	10%	5%	0%	-
Al	<0.13	<0.13	<0.13	<0.13	<0.13	<0.13
Ca	1.70 ± 0.29	2.19 ± 0.15	1.06 ± 0.18	0.61 ± 0.02	<0.13	<0.13
Na	<0.67	<0.67	<0.67	<0.67	<0.67	<0.67
P	2.71 ± 0.01	3.44 ± 0.10	1.59 ± 0.05	1.22 ± 0.03	<0.67	<0.67
Sr	1.24 ± 0.14	1.99 ± 0.73	1.95 ± 1.24	0.85 ± 0.22	<0.13	<0.13

5.7 The inhibition of *S. mutans* growth

The low number of *S. mutans* colony after 48 h of incubation was observed with F1 and F2 (Figure 5-13). The highest and lowest number of the colony was detected with blank control (3.8 ± 0.1 Log CFU/mL) and F2 (2.6 ± 0.3 Log CFU/mL)(Figure 5-14). F2 showed a lower colony than Trans (3.5 ± 0.1 Log CFU/mL) and a significantly lower colony than the blank control ($p < 0.01$). The colony of F1 (2.8 ± 0.1 Log CFU/mL) was comparable to F2 ($p = 0.9466$), but significantly lower than the blank control ($p = 0.0057$).

Factorial analysis showed that the increase in Sr/CaP from 5 to 10 wt% reduced the Log CFU/mL of *S. mutans* by 18 ± 3 %. The increase in Andro from 5 to 10 wt% showed no reduction of *S. mutans*.

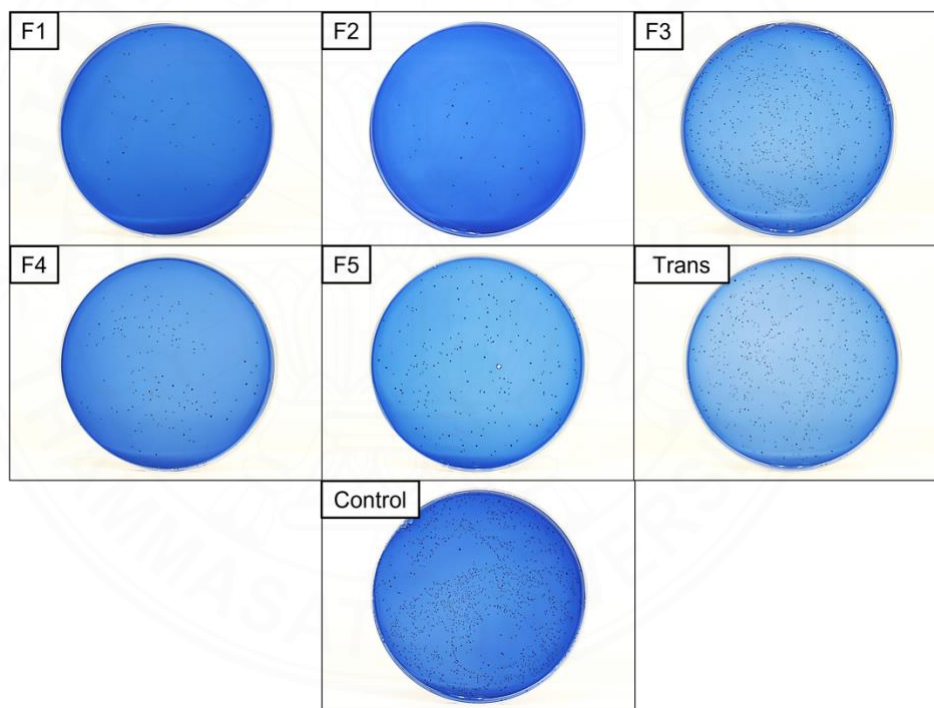


Figure 5-13 Colony-forming unit of samples in each group, which were counted after 48 h of incubation at 37 °C 5 % CO₂ atmosphere.

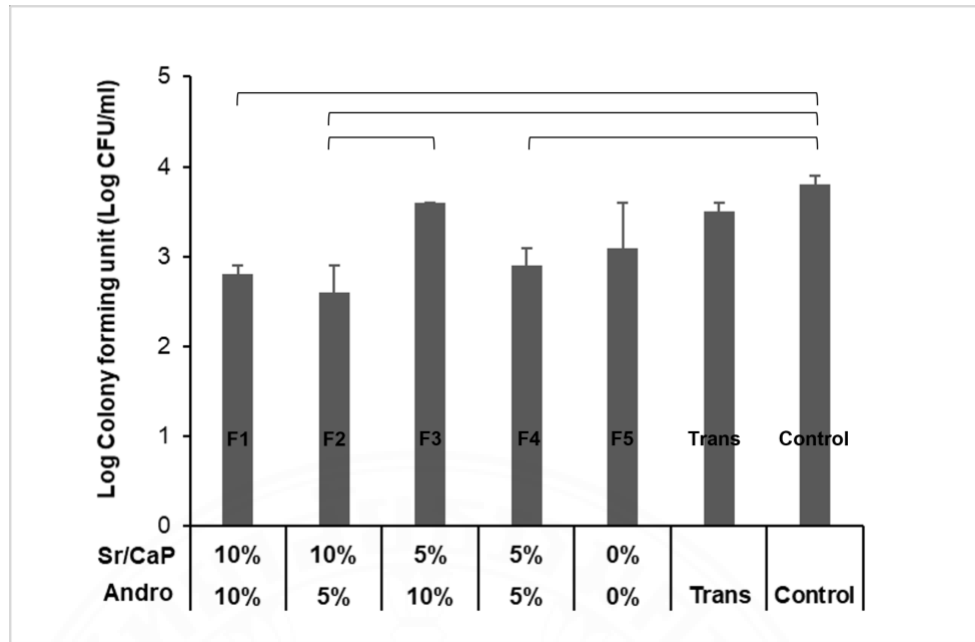


Figure 5-14 The mean of Log colony forming unit per millilitre (Log CFU/mL) of all experimental groups after 48 h of incubation at 37 °C 5 % CO₂ atmosphere. The lines indicate significant differences between groups ($p < 0.05$). Error bars are 95% CI (n = 3).

Chapter 6 Discussion

The aim of the current study was to prepare the experimental orthodontic adhesives containing Sr/CaP and Andro. The effect of increasing Sr/CaP and Andro levels from 5 wt% to 10 wt% was assessed. The second hypothesis was rejected because the rising level of the additives affected water sorption / solubility, biaxial flexural strength and modulus, shear bond strength, mineral precipitation, ion release, and the growth of *S. mutans*. The third hypothesis was also rejected since the results obtained from the experimental adhesives were not comparable to that of the commercial comparison.

6.1 Degree of monomer conversion (DC)

A high degree of monomer conversion is required to reduce the risk of toxic monomers leaching and provide good strength (Aljabo et al., 2015; Kangwankai et al., 2017). The release of unbounded monomers due to the suboptimal polymerization of the orthodontic adhesives may cause toxicity and allergic reaction (Peterson et al., 2017; Sifakakis and Eliades, 2017; Barber and Dhaliwal, 2018; Pelourde et al., 2018). Additionally, the release of unbounded monomers could promote the increase of cariogenic biofilm (Goldberg, 2008).

The results from the studies showed that the additives reduced the degree of monomer conversion of the experimental orthodontic adhesives. The possible explanation could be that the addition of Sr/CaP and Andro introduce the refractive index mismatch that could increase light scattering and reduce light penetration. This may result in a decrease in polymerization at the bottom (Shortall et al., 2008; Panpisut et al., 2016). The higher monomer conversion observed with experimental orthodontic adhesives compared to Trans could be due to the differences of primary methacrylate monomer. The primary base monomer of Trans was bisphenol A-glycidyl methacrylate (Bis-GMA) (Papakonstantinou et al., 2013). It is proposed that the use of monomer that exhibited low glass transition temperature (T_g) usually result in a high level of monomer conversion due to diffusive potential of the base monomers through the resins organic matrix, which could promote polymerization and improves cross-linking of the polymer network (Charton et al., 2007; Walters et al., 2016). The T_g of UDMA (-35.3 °C) is lower than that of Bis-GMA (-7.7 °C), which was the primary base monomer in Trans. Hence, the

monomer conversion of the experimental adhesives was expected to be higher than that of the commercial material (Sideridou et al., 2002; Floyd and Dickens, 2006; Papakonstantinou et al., 2013; Walters et al., 2016).

It was proposed that the resin-based materials with monomer conversion greater than 50 % could reduce the risk of toxic monomers elution. Future works should include elution studies and toxicity tests.

6.2 Water sorption (W_{sp}) and solubility (W_{sl})

It is known that resin-based materials can absorb water from the environment. The absorbed water may cause hygroscopic expansion, hydrolytic degradation, and releasing of the active components (Ferracane, 2006; Malacarne et al., 2006; Panpisut et al., 2016; Spanovic et al., 2019). The excessive water sorption may cause water plasticization, which could subsequently reduce the strength of materials (Ito et al., 2005).

The additives with hydrophilic nature, such as strontium-bioactive glass nanoparticles (SrBGNPs) and monocalcium phosphate monohydrate (MCPM), could be the primary factor that promoted water sorption into the material (Ferracane, 2006; Panpisut et al., 2016; Spanovic et al., 2019). This was reflected by the result from the factorial analysis that the increase of Sr/CaP level significantly increased the level of water sorption of the material. Additionally, the results in the current study suggested the addition of Sr/CaP and Andro for 5 or 10 wt% lead to the increase of water sorption greater than the maximum limit specified by the ISO standard ($< 40 \mu\text{g}/\text{mm}^3$) (British Standard, 2019). The lack of hydrophilic additives in F5 and Trans resulted in an acceptable level of water sorption. However, it is known that water is essential to promote the release of active components from resin-based materials (Chiari et al., 2015; Alania et al., 2016; Kangwankai et al., 2017). Additionally, water sorption may lead to volume expansion of resin-based material, which could help compensate for the polymerization shrinkage stress that occurred within the material (Panpisut et al., 2016; Spanovic et al., 2019; Sawat et al., 2020). Future work should therefore assess the dimensional stability of the material.

The increase in water sorption was expected to enhance the water solubility of the materials. The absorbed water may lead to hydrolytic degradation of methacrylate polymer, which may result in the release of the components from the materials (Chiari et

al., 2015; Alania et al., 2016; Kangwankai et al., 2017). Additionally, SrBG-NPs and MCPM may react with water leading to the release of calcium and phosphate ions from the materials (Chiari et al., 2015; Alania et al., 2016; Panpisut et al., 2016; Elkassas and Arafa, 2017). The result from the current study demonstrated that the water solubility of all experimental adhesives was within the range of that required by the BS ISO 4049 ($< 7.5 \mu\text{g}/\text{mm}^3$) (British Standard, 2019).

Previous studies demonstrated that the addition of MCPM promoted the ion release and the formation of calcium phosphate fillers such as dicalcium phosphate dihydrate (DCPD), which contain water in the structure. The formation of higher density dicalcium phosphate may therefore compensate for the weight loss from the material (Kangwankai et al., 2017; Sawat et al., 2020). The other possible reasons for the low solubility of the materials could be due to the slow degradation of strontium-bioactive glass nanoparticles and low water solubility of andrographolide (Ren et al., 2009; Aromdee, 2012; Spanovic et al., 2019). Additionally, the high level of degree of monomer conversion may reduce uncured monomers release. This may reduce the loss of mass from the materials.

6.3 Biaxial flexural strength (BFS) and Biaxial flexural modulus (BFM)

High mechanical properties of materials are believed to help ensure that the materials can withstand the applied forces. The requirement of flexural strength for resin-based material for luting purposes in the ISO 4049 was 50 MPa (British Standard, 2019). Hence, this may suggest that the experimental adhesives would pass the standard. Sr/CaP and Andro were not silanized to promote the release of the reactive components. The experimental formulation containing additives of the experimental orthodontic adhesives contained inert glass from 40 - 45 wt%.

The method of replacing the additive with inert glass was commonly used to facilitate and simplify the preparation process of novel resin composite-based materials for manufacturers. The effect from reducing glass levels for up to 10 wt% was dominated by the effect from the addition of hydrophilic additives (Chatzistavrou et al., 2015; Aljabo et al., 2016; Khvostenko et al., 2016; Panpisut et al., 2016; Yang et al., 2016; Kangwankai et al., 2017; Panpisut et al., 2019).

The addition of Sr/CaP and Andro reduced the strength of materials as was expected. The non-silanated surfaces may introduce weak interfaces between the fillers and the polymer phase in the experimental adhesives (Kangwankai et al., 2017). The increase in water sorption due to the hydrophilic additive fillers may additionally increase water plasticization, which reduces the rigidity and mechanical strength of the polymer network (Aljabo et al., 2015; Chiari et al., 2015). The increase of Sr/CaP showed minimal effect on the strength compared to that of the increase of Andro. The possible explanation could be due to the average size of fillers of SrBGNPs (~ 200 nm) and MCPM (~ 10 µm), which was smaller than that of Andro (10 – 50 µm). It was demonstrated that the use of smaller fillers in composites exhibited higher strength than the use of larger fillers (Fu et al., 2008).

It should be mentioned that the current study employed biaxial flexural strength instead of a 3-point bending test in the ISO 4049:2019 Dentistry-Polymer-based restorative materials (British Standard, 2019). The use of BFS testing requires fewer materials and the specimen preparation was less complicated compared to that of the 3-point bending test. The guideline for material testing also demonstrated that the result obtained from the biaxial flexural test was comparable to that of 3-point bending but with greater reproducibility (Ilie et al., 2017). The 3-point bending test may be used when the optimization step is completed, and the final formulation is obtained.

6.4 Enamel shear bond strength (SBS) and Adhesive remnant index (ARI)

The high bond strength between the adhesive and enamel is essential to ensure the active force from the archwire can be transferred to the anchored tooth without dislodgement (Sharma et al., 2014; Zhang et al., 2016). The high variation of SBS was commonly observed due to the different compositions among the extracted teeth and the sensitive technique for specimen preparation.

The shear bond strength of the experimental adhesives was within the range of that reported with the published studies (24.4 – 3.9 MPa)(Akhavan et al., 2013; Sharma et al., 2014). The observed shear bond strength of the experimental adhesive containing Sr/CaP and Andro was lower than that of Trans. This could be due to the lack of silanization of

the additives or the hydrophilicity of Sr/CaP (Aljabo et al., 2015; Chiari et al., 2015; Kangwankai et al., 2017). It should be mentioned that the effect of increasing Sr/CaP level on strength reduction was detected with shear bond strength but not the biaxial flexural strength. It is possible that the thermocycling process in the shear bond strength test may accelerate the degradation and dissolution of SrBGNPs and MCPM, thereby affecting the strength of the materials (Lopes et al., 2020).

Currently, there are no minimum requirements specified by the ISO for the SBS of orthodontic adhesives. The SBS of the experimental adhesives exhibited the SBS values greater than the clinically acceptable level (~ 8 MPa) which previously reported in the published studies (Reynolds, 1975; Bishara et al., 2007). Additionally, the lower shear bond strength of experimental adhesives compared with Trans may facilitate the orthodontic bracket debonding process and might prevent enamel from possible damage (Degrazia et al., 2016). The bond strength of the orthodontic adhesive can be reduced by the degradation from the bacterial biofilm. Future work may consider assessing the effect of biofilm on the shear bond strength of the experimental materials.

The adhesive remnant index (ARI) is one of the most commonly used methods of assessing the quality of adhesion between the composite and tooth as well as between the composite and bracket base (Sharma et al., 2014). Generally, the failure within the adhesive layer, which leaving remnants of adhesive on the enamel surface, may help protect the enamel surface (Bishara et al., 2007; Yang et al., 2016). A high ARI score may suggest the strong bond between adhesive and enamel surface, which may result in the destruction of enamel during debonding process (Sharma et al., 2014; Yang et al., 2016). Hence, a low ARI score may be preferable to reduce the risk of enamel breakdown after debonding. The ARI of score 0 or 1 was commonly obtained from experimental adhesive and Trans, which could be clinically advantageous (Bishara et al., 2007).

6.5 Mineral precipitation

The release of ions from the orthodontic adhesives was expected to promote remineralization in the incipient caries lesions (white spot lesions) (Aljabo et al., 2016; Panpisut et al., 2016; Kangwankai et al., 2017). The essential ions for hydroxyapatite precipitation are calcium and phosphate ions. The study demonstrated that resin-based

materials that can release ions to promote calcium phosphate precipitation showed the remineralizing effects in carious lesions (Li et al., 2014). Additionally, it was demonstrated that strontium (Sr) could enhance apatite precipitation by stabilizing the nucleation of apatite formation (Pan et al., 2009; Schumacher and Gelinsky, 2015).

The addition of Sr/CaP fillers promoted the release of Ca, P, and Sr. The increase in ions concentration and suitable pH are needed to encourage mineral precipitation (Xu et al., 2009). This may be indicated that the additive releases ions and promote a suitable environment for the precipitation of calcium phosphate apatite.

The Ca/P atomic ratio of the precipitate could be used to initially identify the calcium phosphate species that were precipitated. The EDX results showed that the Ca/P ratio of the precipitate was ~ 0.5 , which was much lower than that of hydroxyapatite (Ca/P ratio of 1.67). The possible explanation could be that the precipitate was in the early stage of crystal formation since the immersion time of the specimen was only 24 h. It was demonstrated that hydroxyapatite was detected on the orthodontic adhesive containing bioactive glass after immersion in artificial saliva for 6 months (Al-Eesa et al., 2019). Additionally, future work should be focused on the remineralizing effect at the tooth-adhesive interface in the biofilm model.

6.6 Ion release

The addition of MCPM and SrBGNPs are expected to promote ion release for enhancing the mineralizing effects for the experimental orthodontic adhesives. The addition of Sr/CaP (SrBGNPs + MCPM) promoted Ca, P, and Sr release from the experimental adhesives as was expected. This may suggest that the experimental adhesives exhibit ion-releasing properties, which could potentially promote the remineralizing effects for the caries lesions (Li et al., 2014).

The rising level of Sr/CaP increased the level of ion release as was expected. Hence, SrBGNPs combined with MCPM may be considered as excellent ion releasing fillers for dental applications. The beneficial effect of Sr release includes mineralizing and antibacterial actions (Liu et al., 2016). It was suggested that Sr enhance calcium phosphate apatite formation by increasing the amount of nucleation cluster of apatite (Pan et al., 2009; Schumacher and Gelinsky, 2015). Additionally, the Sr may exhibit some

inhibitory effect on bacteria (Liu et al., 2016; Dai et al., 2020). The limitation of the study was that the release was measured at the final time point. The measurement of ion release in the future study could be performed at different time points to assess the releasing kinetic of ions.

6.7 The inhibition of *S. mutans* growth

The antibacterial actions of orthodontics adhesives may help inhibit the growth of cariogenic biofilm, which could subsequently reduce the risk of incipient caries formation. The antibacterial action of the current study was tested as an indirect antibacterial action since the bacteria were cultured with the media containing extract from the specimens (Ferreira et al., 2019).

The increase in the level of Sr/CaP from 5 to 10 wt% enhance the antibacterial actions of the experimental orthodontic adhesives. The effect was expected to be due to Strontium-bioactive glass nanoparticles (SrBGNPs). This was in accordance with the previous studies, which demonstrated the antibacterial actions of the SrBGNPs (Chatzistavrou et al., 2015; Xu et al., 2015; Liu et al., 2016). The actual antibacterial mechanism of the strontium is not yet concluded (Liu et al., 2016). It can be hypothesized that the bioactive glass nanoparticles may release from the adhesive and penetrate into the bacterial cell due to its nanosize (Elkassas and Arafa, 2017). This may alter the intracellular pH and the osmotic pressure which may affect bacterial cell viability (Martins et al., 2011; Xu et al., 2015). The addition of Andro nor the increasing level of Andro was not associated with the increase in antibacterial actions. The possible explanation could be the low water-soluble of Andro, which may limit the release of Andro from the adhesives (Gupta et al., 2017; Gaur et al., 2018; Mussard et al., 2019). The future antibacterial test could be focused on the direct contact antibacterial test. Additionally, the effect of Andro was associated with the reduction of bacterial adhesion and the inhibition of biofilm formation (Limsong et al., 2004; Li et al., 2006; Banerjee et al., 2017). The assessment of cariogenic biofilm cultured on the materials should be investigated in future studies.

6.8 The summary of the additive effects of this current study was exhibited in the Table 6-1.

Table 6-1 The summary of the additive effects.

Tests		Increasing of Sr/CaP (↑)	Increasing of Andro (↑)
Degree of monomer conversion (%)		Non	Non
Water sorption ($\mu\text{g}/\text{mm}^3$)		↑	Non
Water solubility ($\mu\text{g}/\text{mm}^3$)		Non	↑
Biaxial flexural strength / modulus (MPa, GPa)		Non	↓
Enamel shear bond strength (MPa)		↓	Non
Adhesive remnant area (%)		Non	Non
Mineral precipitation (Yes / No)		Yes	Non
Ions release (ppm)	Ca	↑	Non
	P	↑	Non
	Sr	Non	Non
The inhibition of <i>S. mutans</i> growth (Log CFU/mL)		↓	Non

6.9 Future works

The major fields that should be investigated in future projects are as follows.

- Degree of monomer conversion with short light-curing time (< 20 s).
- Long-term mechanical properties and the dimensional stability of the material.
- Enamel shear bond strength after longer-term immersion / thermocycling period.
- Effect of biofilm on the shear bond strength of the experimental materials.
- Identification of unknown crystalline materials using X-ray diffraction (XRD) and Raman microscope.

- Remineralizing effect at the tooth-adhesive interface in the biofilm model.
- Measurement of ion release which performed at different time points to assess the releasing kinetic of ions.
- Assessment of biofilm growth on the materials using live and dead assay.

6.10 Limitation

- This study is *in vitro* study; therefore, the clinical relevance should be carefully interpreted.
- The flexural test was a short-term study (24 h BFS).
- The apatite formation was not confirmed with conventional spectroscopic techniques such as XRD, Raman microscope.
- The materials were hand-mixed, so the quality of mixing of each batch may be different.

Chapter 7 Conclusions

Within the limitation of the current study, the following conclusion can be drawn.

- The ion releasing and antibacterial experimental orthodontic adhesives containing Sr/CaP and Andro were prepared. The additives reduced the physical and mechanical properties of the experimental adhesives.
- The increase of Sr/CaP level from 5 to 10 wt% showed minimal effect on the degree of monomer conversion, biaxial flexural strength / modulus. Rising Sr/CaP increased water sorption and ion release but reduced the shear bond strength of the materials. The addition of Sr/CaP promoted Ca, P ions release and the formation of calcium phosphate precipitation. The increase of Sr/CaP level inhibited the growth of *S. mutans*.
- The increase in Andro level from 5 to 10 wt% showed negligible effect on monomer conversion and water sorption but reduced biaxial flexural strength / modulus of the materials. The increase of Andro did not inhibit the growth of *S. mutans*.
- The experimental adhesives that contain additives presented similar degree of monomer conversion and SBS to the commercial material. Water sorption and water solubility of the experimental adhesives with additives were higher than those of the commercial material. The strength of the experimental materials containing additives was lower than the commercial material, but the values were still in the acceptable range. The adhesives exhibited ion release and calcium phosphate precipitation which were not detected from the commercial material. The adhesives with high level of SrBGNPs reduced the growth of *S. mutans* which was much lower than that of the blank control compared with the commercial material.

The ability of the experimental adhesive to promote ion release, mineral precipitation, and the inhibition of *S. mutans* is promising to inhibit caries, prevent demineralization, and promote remineralization of enamel. This could potentially help to reduce the development of white spot lesions.

Chapter 8 References

- Abreu L. G., 2018. Orthodontics in Children and Impact of Malocclusion on Adolescents' Quality of Life. *Pediatric Clinics*. 65 (5), 995-1006.
- Ajita J., Saravanan S. & Selvamurugan N., 2015. Effect of size of bioactive glass nanoparticles on mesenchymal stem cell proliferation for dental and orthopedic applications. *Materials Science and Engineering: C*. 53 142-149.
- Akhavan A., Sodagar A., Mojtahedzadeh F. & Sodagar K., 2013. Investigating the effect of incorporating nanosilver/nanohydroxyapatite particles on the shear bond strength of orthodontic adhesives. *Acta Odontol Scand*. 71 (5), 1038-42.
- Al Maaitah E. F., Adeyemi A. A., Higham S. M., Pender N. & Harrison J. E., 2011. Factors affecting demineralization during orthodontic treatment: a post-hoc analysis of RCT recruits. *American Journal of Orthodontics and Dentofacial Orthopedics*. 139 (2), 181-191.
- Al Maaitah E. F., Omar A. a. A. & Al-Khateeb S. N., 2013. Effect of fixed orthodontic appliances bonded with different etching techniques on tooth color: a prospective clinical study. *American Journal of Orthodontics and Dentofacial Orthopedics*. 144 (1), 43-49.
- Al-Eesa N., Johal A., Hill R. & Wong F., 2018. Fluoride containing bioactive glass composite for orthodontic adhesives—Apatite formation properties. *Dental Materials*. 34 (8), 1127-1133.
- Al-Eesa N., Wong F., Johal A. & Hill R., 2017. Fluoride containing bioactive glass composite for orthodontic adhesives—ion release properties. *Dental Materials*. 33 (11), 1324-1329.
- Al-Eesa N. A., Karpukhina N., Hill R. G., Johal A. & Wong F. S. L., 2019. Bioactive glass composite for orthodontic adhesives - Formation and characterisation of apatites using MAS-NMR and SEM. *Dent Mater*. 35 (4), 597-605.
- Alania Y., Chiari M. D., Rodrigues M. C., Arana-Chavez V. E., Bressiani A. H. A., Vichi F. M., et al., 2016. Bioactive composites containing TEGDMA-functionalized calcium phosphate particles: degree of conversion, fracture strength and ion release evaluation. *Dental Materials*. 32 (12), e374-e381.
- Aljabo A., Abou Neel E. A., Knowles J. C. & Young A. M., 2016. Development of dental composites with reactive fillers that promote precipitation of antibacterial-hydroxyapatite layers. *Materials Science and Engineering: C*. 60 285-292.
- Aljabo A., Xia W., Liaqat S., Khan M., Knowles J., Ashley P., et al., 2015. Conversion, shrinkage, water sorption, flexural strength and modulus of re-mineralizing dental composites. *Dental Materials*. 31 (11), 1279-1289.

- Alshali R. Z., Salim N. A., Satterthwaite J. D. & Silikas N., 2015. Long-term sorption and solubility of bulk-fill and conventional resin-composites in water and artificial saliva. *Journal of Dentistry*. 43 (12), 1511-1518.
- Arifullah M., Namsa N. D., Mandal M., Chiruvella K. K., Vikrama P. & Gopal G. R., 2013. Evaluation of anti-bacterial and anti-oxidant potential of andrographolide and echiodinin isolated from callus culture of *Andrographis paniculata* Nees. *Asian Pacific journal of tropical biomedicine*. 3 (8), 604-610.
- Aromdee C., 2012. Modifications of andrographolide to increase some biological activities: a patent review (2006–2011). *Expert opinion on therapeutic patents*. 22 (2), 169-180.
- Badawi H., Evans R., Wilson M., Ready D., Noar J. & Pratten J., 2003. The effect of orthodontic bonding materials on dental plaque accumulation and composition in vitro. *Biomaterials*. 24 (19), 3345-3350.
- Baker C., Pradhan A., Pakstis L., Pochan D. J. & Shah S. I., 2005. Synthesis and antibacterial properties of silver nanoparticles. *Journal of nanoscience and nanotechnology*. 5 (2), 244-249.
- Bakry A. S., Marghalani H. Y., Amin O. A. & Tagami J., 2014. The effect of a bioglass paste on enamel exposed to erosive challenge. *Journal of Dentistry*. 42 (11), 1458-1463.
- Banerjee M., Parai D., Chattopadhyay S. & Mukherjee S. K., 2017. Andrographolide: antibacterial activity against common bacteria of human health concern and possible mechanism of action. *Folia microbiologica*. 62 (3), 237-244.
- Barber S. K. & Dhaliwal H. K., 2018. Allergy to acrylate in composite in an orthodontic patient: a case report. *Journal of orthodontics*. 45 (3), 203-209.
- Beerens M. W., Boekitwetan F., Van Der Veen M. H. & Ten Cate J. M., 2015. White spot lesions after orthodontic treatment assessed by clinical photographs and by quantitative light-induced fluorescence imaging; a retrospective study. *Acta Odontologica Scandinavica*. 73 (6), 441-446.
- Beltrami R., Chiesa M., Scribante A., Allegretti J. & Poggio C., 2016. Comparison of shear bond strength of universal adhesives on etched and nonetched enamel. *Journal of applied biomaterials & functional materials*. 14 (1), 78-83.
- Benson P. E., Alexander-Abt J., Cotter S., Dyer F. M., Fenesha F., Patel A., et al., 2019. Resin-modified glass ionomer cement vs composite for orthodontic bonding: A multicenter, single-blind, randomized controlled trial. *American Journal of Orthodontics and Dentofacial Orthopedics*. 155 (1), 10-18.
- Bishara S. E., Ostby A. W., Laffoon J. F. & Warren J., 2007. Shear bond strength comparison of two adhesive systems following thermocycling: a new self-etch primer and a resin-modified glass ionomer. *The Angle Orthodontist*. 77 (2), 337-341.

- Brauer D. S., Karpukhina N., O'donnell M. D., Law R. V. & Hill R. G., 2010. Fluoride-containing bioactive glasses: effect of glass design and structure on degradation, pH and apatite formation in simulated body fluid. *Acta biomaterialia*. 6 (8), 3275-3282.
- British Standard 2019. BS EN ISO 4049:2019. *Dentistry-Polymer- based restorative materials*. Switzerland: BSI Standards.
- Bucur S. M., Cocos D. & Saghin A., 2020. Bond strength of three adhesive systems used for bonding orthodontic brackets. *Romanian Journal of Oral Rehabilitation*. 12 (1), 162-7.
- Burwell A., Litkowski L. & Greenspan D., 2009. Calcium sodium phosphosilicate (NovaMin®): remineralization potential. *Advances in Dental Research*. 21 (1), 35-39.
- Carvalho S. M., Moreira C. D., Oliveira A. C. X., Oliveira A. A., Lemos E. M. & Pereira M. M. 2019. Bioactive glass nanoparticles for periodontal regeneration and applications in dentistry. *Nanobiomaterials in clinical dentistry*. Elsevier, 351-383.
- Chambers C., Stewart S., Su B., Sandy J. & Ireland A., 2013. Prevention and treatment of demineralisation during fixed appliance therapy: a review of current methods and future applications. *British dental journal*. 215 (10), 505-511.
- Chapman J. A., Roberts W. E., Eckert G. J., Kula K. S. & González-Cabezas C., 2010. Risk factors for incidence and severity of white spot lesions during treatment with fixed orthodontic appliances. *American Journal of Orthodontics and Dentofacial Orthopedics*. 138 (2), 188-194.
- Charton C., Falk V., Marchal P., Pla F. & Colon P., 2007. Influence of Tg, viscosity and chemical structure of monomers on shrinkage stress in light-cured dimethacrylate-based dental resins. *Dental Materials*. 23 (11), 1447-1459.
- Chatzistavrou X., Velamakanni S., Drenzo K., Lefkelidou A., Fenno J. C., Kasuga T., et al., 2015. Designing dental composites with bioactive and bactericidal properties. *Materials Science and Engineering: C*. 52 267-272.
- Cheng L., Zhang K., Melo M. A., Weir M., Zhou X. & Xu H., 2012. Anti-biofilm dentin primer with quaternary ammonium and silver nanoparticles. *Journal of dental research*. 91 (6), 598-604.
- Cheng L., Zhang K., Zhou C.-C., Weir M. D., Zhou X.-D. & Xu H. H., 2016. One-year water-ageing of calcium phosphate composite containing nano-silver and quaternary ammonium to inhibit biofilms. *International journal of oral science*. 8 (3), 172-181.
- Chiari M. D., Rodrigues M. C., Xavier T. A., De Souza E. M., Arana-Chavez V. E. & Braga R. R., 2015. Mechanical properties and ion release from bioactive restorative composites containing glass fillers and calcium phosphate nano-structured particles. *Dental Materials*. 31 (6), 726-733.

- Chuacharoen D., 2014. The relationship between demand and need for orthodontic treatment in high school students in Bangkok. *Journal of the medical association of Thailand*. 97 (7), 758-66.
- Dai L. L., Mei M. L., Chu C. H. & Lo E. C. M., 2020. Antibacterial effect of a new bioactive glass on cariogenic bacteria. *Archives of Oral Biology*. 117 104833.
- Degrazia F. W., Leitune V. C. B., Garcia I. M., Arthur R. A., Samuel S. M. W. & Collares F. M., 2016. Effect of silver nanoparticles on the physicochemical and antimicrobial properties of an orthodontic adhesive. *Journal of Applied Oral Science*. 24 404-410.
- Derks A., Katsaros C., Frencken J., Van't Hof M. & Kuijpers-Jagtman A., 2004. Caries-inhibiting effect of preventive measures during orthodontic treatment with fixed appliances. *Caries research*. 38 (5), 413-420.
- Dimberg L., Arnrup K. & Bondemark L., 2015. The impact of malocclusion on the quality of life among children and adolescents: a systematic review of quantitative studies. *European Journal of Orthodontics*. 37 (3), 238-247.
- Dorozhkin S. V. & Epple M., 2002. Biological and medical significance of calcium phosphates. *Angewandte Chemie International Edition*. 41 (17), 3130-3146.
- Dziuk Y., Chhatwani S., Möhlhenrich S. C., Tulka S., Naumova E. A. & Danesh G., 2021. Fluoride release from two types of fluoride-containing orthodontic adhesives: Conventional versus resin-modified glass ionomer cements—An in vitro study. *PloS one*. 16 (2), e0247716.
- Elkassas D. & Arafa A., 2017. The innovative applications of therapeutic nanostructures in dentistry. *Nanomedicine: Nanotechnology, Biology and Medicine*. 13 (4), 1543-1562.
- Erol - Taygun M., Zheng K. & Boccaccini A. R., 2013. Nanoscale bioactive glasses in medical applications. *International Journal of Applied Glass Science*. 4 (2), 136-148.
- Eslamian L., Borzabadi-Farahani A., Karimi S., Saadat S. & Badiie M. R., 2020. Evaluation of the shear bond strength and antibacterial activity of orthodontic adhesive containing silver nanoparticle, an in-vitro study. *Nanomaterials*. 10 (8), 1466.
- Fernando D., Attik N., Pradelle-Plasse N., Jackson P., Grosgeat B. & Colon P., 2017. Bioactive glass for dentin remineralization: A systematic review. *Materials Science and Engineering: C*. 76 1369-1377.
- Ferracane J. L. J. D. M., 2006. Hygroscopic and hydrolytic effects in dental polymer networks. 22 (3), 211-222.
- Ferreira C. J., Leitune V. C. B., Balbinot G. D. S., Degrazia F. W., Arakelyan M., Sauro S., et al., 2019. Antibacterial and remineralizing fillers in experimental orthodontic adhesives. *Materials*. 12 (4), 652.

- Floyd C. J. & Dickens S. H. J. D. M., 2006. Network structure of Bis-GMA-and UDMA-based resin systems. 22 (12), 1143-1149.
- Fredholm Y. C., Karpukhina N., Brauer D. S., Jones J. R., Law R. V. & Hill R. G., 2011. Influence of strontium for calcium substitution in bioactive glasses on degradation, ion release and apatite formation. *Journal of the royal society interface*. 9 (70), 880-889.
- Fredholm Y. C., Karpukhina N., Law R. V. & Hill R. G., 2010. Strontium containing bioactive glasses: glass structure and physical properties. *Journal of Non-Crystalline Solids*. 356 (44-49), 2546-2551.
- Fu S. Y., Feng X. Q., Lauke B. & Mai Y. W., 2008. Effects of particle size, particle/matrix interface adhesion and particle loading on mechanical properties of particulate-polymer composites. *Compos B Eng*. 39 (6), 933-961.
- Gange P., 2015. The evolution of bonding in orthodontics. *American Journal of Orthodontics and Dentofacial Orthopedics*. 147 (4), S56-S63.
- Gaur P., Sharma S., Pandey S., Bhattacharya S. & Kant S., 2018. Pharmacological and Clinical Effects of *Andrographis paniculata*. *International journal of life sciences research*. 2455 (1716), 1716.
- Goldberg M., 2008. In vitro and in vivo studies on the toxicity of dental resin components: a review. *Clinical oral investigations*. 12 (1), 1-8.
- Goldberg M. 2016. Enamel Etching. *Understanding dental caries*. Springer, 19-27.
- Gorton J. & Featherstone J. D., 2003. In vivo inhibition of demineralization around orthodontic brackets. *American Journal of Orthodontics and Dentofacial Orthopedics*. 123 (1), 10-14.
- Guerra F., Mazur M., Nardi G. M., Corridore D., Pasqualotto D., Rinado F., et al., 2015. Dental hypomineralized enamel resin infiltration. Clinical indications and limits. *Senses and Sciences*. 2 (4).
- Gupta S., Mishra K. & Ganju L., 2017. Broad-spectrum antiviral properties of andrographolide. *Archives of virology*. 162 (3), 611-623.
- Heymann G. C. & Grauer D., 2013. A contemporary review of white spot lesions in orthodontics. *Journal of Esthetic and Restorative Dentistry*. 25 (2), 85-95.
- Hobley L., Harkins C., Macphee C. E. & Stanley-Wall N. R., 2015. Giving structure to the biofilm matrix: an overview of individual strategies and emerging common themes. *FEMS microbiology reviews*. 39 (5), 649-669.
- Höchli D., Hersberger-Zurfluh M., Papageorgiou S. N. & Eliades T., 2016. Interventions for orthodontically induced white spot lesions: a systematic review and meta-analysis. *European Journal of Orthodontics*. 39 (2), 122-133.

- Ilie N., Hilton T., Heintze S., Hickel R., Watts D., Silikas N., et al., 2017. Academy of dental materials guidance—resin composites: Part I—mechanical properties. *Dental Materials*. 33 (8), 880-894.
- Ito S., Hashimoto M., Wadgaonkar B., Svizero N., Carvalho R. M., Yiu C., et al., 2005. Effects of resin hydrophilicity on water sorption and changes in modulus of elasticity. *Biomaterials*. 26 (33), 6449-6459.
- Jiang X., Yu P., Jiang J., Zhang Z., Wang Z., Yang Z., et al., 2009. Synthesis and evaluation of antibacterial activities of andrographolide analogues. *European journal of medicinal chemistry*. 44 (7), 2936-2943.
- Kangwankai K., Sani S., Panpisut P., Xia W., Ashley P., Petridis H., et al., 2017. Monomer conversion, dimensional stability, strength, modulus, surface apatite precipitation and wear of novel, reactive calcium phosphate and polylysine-containing dental composites. *PloS one*. 12 (11).
- Kaur G., Pandey O. P., Singh K., Homa D., Scott B. & Pickrell G., 2014. A review of bioactive glasses: their structure, properties, fabrication and apatite formation. *Journal of biomedical materials research*. 102 (1), 254-274.
- Kazancı F., Aydoğan C. & Alkan Ö., 2016. Patients' and parents' concerns and decisions about orthodontic treatment. *The Korean Journal of Orthodontics*. 46 (1), 20-26.
- Kerbusch A. E., Kuijpers-Jagtman A. M., Mulder J. & Sanden W. J. V. D., 2012. Methods used for prevention of white spot lesion development during orthodontic treatment with fixed appliances. *Acta Odontologica Scandinavica*. 70 (6), 564-568.
- Khvostenko D., Hilton T., Ferracane J., Mitchell J. & Kruzic J., 2016. Bioactive glass fillers reduce bacterial penetration into marginal gaps for composite restorations. *Dental Materials*. 32 (1), 73-81.
- Klein M. I., Hwang G., Santos P. H., Campanella O. H. & Koo H., 2015. Streptococcus mutans-derived extracellular matrix in cariogenic oral biofilms. *Frontiers in cellular and infection microbiology*. 5 10.
- Li F., Wang P., Weir M. D., Fouad A. F. & Xu H. H., 2014. Evaluation of antibacterial and remineralizing nanocomposite and adhesive in rat tooth cavity model. *Acta biomaterialia*. 10 (6), 2804-2813.
- Li H., Qin H., Wang W., Li G., Wu C. & Song J., 2006. Effect of andrographolide on QS regulating virulence factors production in *Pseudomonas aeruginosa*. *China journal of Chinese materia medica*. 31 (12), 1015-1017.
- Limsong J., Benjavongkulchai E. & Kuvatanasuchati J., 2004. Inhibitory effect of some herbal extracts on adherence of *Streptococcus mutans*. *Journal of ethnopharmacology*. 92 (2-3), 281-289.

- Liu J., Rawlinson S. C., Hill R. G. & Fortune F., 2016. Strontium-substituted bioactive glasses in vitro osteogenic and antibacterial effects. *Dental Materials*. 32 (3), 412-422.
- Liu J. L., Luo Z. & Bashir S., 2013. A progressive approach on inactivation of bacteria using silver–titania nanoparticles. *Biomaterials science*. 1 (2), 194-201.
- Lopatiene K., Borisovaite M. & Lapenaite E., 2016. Prevention and treatment of white spot lesions during and after treatment with fixed orthodontic appliances: a systematic literature review. *Journal of oral & maxillofacial research*. 7 (2).
- Lopes G. V., Correr-Sobrinho L., Correr A. B., Godoi A. P. T. D., Vedovello S. a. S. & Menezes C. C. D., 2020. Light activation and thermocycling methods on the shear bond strength of brackets bonded to porcelain surfaces. *Brazilian dental journal*. 31 52-56.
- Low M., Khoo C. S., Munch G., Govindaraghavan S. & Sucher N. J., 2015. An in vitro study of anti-inflammatory activity of standardised *Andrographis paniculata* extracts and pure andrographolide. *BMC complementary medicine and therapies*. 15 18.
- Lucchese A., Bondemark L., Marcolina M. & Manuelli M., 2018. Changes in oral microbiota due to orthodontic appliances: a systematic review. *Journal of Oral Microbiology*. 10 (1), 1476645.
- Malacarne J., Carvalho R. M., Mario F., Svizero N., Pashley D. H., Tay F. R., et al., 2006. Water sorption/solubility of dental adhesive resins. *Dental Materials*. 22 (10), 973-980.
- Martins C. H. G., Carvalho T. C., Souza M. G. M., Ravagnani C., Peitl O., Zanotto E. D., et al., 2011. Assessment of antimicrobial effect of Biosilicate® against anaerobic, microaerophilic and facultative anaerobic microorganisms. *Journal of Materials Science: Materials in Medicine*. 22 (6), 1439-1446.
- Mehdawi I. M., Pratten J., Spratt D. A., Knowles J. C. & Young A. M., 2013. High strength remineralizing, antibacterial dental composites with reactive calcium phosphates. *Dental Materials*. 29 (4), 473-484.
- Mei L., Chieng J., Wong C., Benic G. & Farella M., 2017. Factors affecting dental biofilm in patients wearing fixed orthodontic appliances. *Progress in orthodontics*. 18 (1), 1-6.
- Melo M. A., Guedes S. F., Xu H. H. & Rodrigues L. K., 2013. Nanotechnology-based restorative materials for dental caries management. *Trends in biotechnology*. 31 (8), 459-467.
- Melo M. A., Wu J., Weir M. D. & Xu H. H., 2014. Novel antibacterial orthodontic cement containing quaternary ammonium monomer dimethylaminododecyl methacrylate. *Journal of Dentistry*. 42 (9), 1193-1201.
- Müller L. K., Jungbauer G., Jungbauer R., Wolf M. & Deschner J., 2021. Biofilm and orthodontic therapy. *Oral Biofilms*. 29 201-213.

- Mummolo S., Tieri M., Nota A., Caruso S., Darvizeh A., Albani F., et al., 2020. Salivary concentrations of *Streptococcus mutans* and *Lactobacilli* during an orthodontic treatment. An observational study comparing fixed and removable orthodontic appliances. *Clinical and experimental dental research*. 6 (2), 181-187.
- Mussard E., Cesaro A., Lespessailles E., Legrain B., Berteina-Raboin S. & Toumi H., 2019. Andrographolide, a natural antioxidant: an update. *Antioxidants*. 8 (12), 571.
- Nam H.-J., Kim Y.-M., Kwon Y. H., Yoo K.-H., Yoon S.-Y., Kim I.-R., et al., 2019. Fluorinated bioactive glass nanoparticles: enamel demineralization prevention and antibacterial effect of orthodontic bonding resin. *Materials*. 12 (11), 1813.
- Pan H.-B., Li Z.-Y., Wang T., Lam W., Wong C., Darvell B., et al., 2009. Nucleation of strontium-substituted apatite. *Crystal Growth and Design*. 9 (8), 3342-3345.
- Panpisut P., Khan M. A., Main K., Arshad M., Xia W., Petridis H., et al., 2019. Polymerization kinetics stability, volumetric changes, apatite precipitation, strontium release and fatigue of novel bone composites for vertebroplasty. *PloS one*. 14 (3), e0207965.
- Panpisut P., Liaqat S., Zacharaki E., Xia W., Petridis H. & Young A. M., 2016. Dental composites with calcium/strontium phosphates and polylysine. *PloS one*. 11 (10), e0164653.
- Papakonstantinou A. E., Eliades T., Cellesi F., Watts D. C. & Silikas N., 2013. Evaluation of UDMA's potential as a substitute for Bis-GMA in orthodontic adhesives. *Dental Materials*. 29 (8), 898-905.
- Park H.-J., Park S., Roh J., Kim S., Choi K., Yi J., et al., 2013. Biofilm-inactivating activity of silver nanoparticles: a comparison with silver ions. *Journal of Industrial and Engineering Chemistry*. 19 (2), 614-619.
- Paula A. B. P., Fernandes A. R., Coelho A. S., Marto C. M., Ferreira M. M., Caramelo F., et al., 2017. Therapies for white spot lesions—a systematic review. *Journal of Evidence Based Dental Practice*. 17 (1), 23-38.
- Pelourde C., Bationo R., Boileau M.-J., Colat-Parros J. & Jordana F., 2018. Monomer release from orthodontic retentions: An in vitro study. *American Journal of Orthodontics and Dentofacial Orthopedics*. 153 (2), 248-254.
- Pemberton M. N., 2016. Allergy to chlorhexidine. *Dental update*. 43 (3), 272-274.
- Peterson M. R., Wong P. H., Dickson S. D. & Coop C. A., 2017. Allergic stomatitis from orthodontic adhesives. *Military medicine*. 182 (3-4), e1883-e1885.
- Pinto A. S., Alves L. S., Maltz M. & Zenkner J. E. D. A., 2020. Association between fixed orthodontic treatment and dental caries: a 1-year longitudinal study. *Brazilian Oral Research*. 35.

- Ren K., Zhang Z., Li Y., Liu J., Zhao D., Zhao Y., et al., 2009. Physicochemical characteristics and oral bioavailability of andrographolide complexed with hydroxypropyl-beta-cyclodextrin. *Die Pharmazie*. 64 (8), 515-20.
- Reynolds I. J. B. J. O. O., 1975. A review of direct orthodontic bonding. 2 (3), 171-178.
- Sawat P., Kitsahawong K., Young A. M., Ashley P. & Pungchanchaikul P. Evaluation of interface between tooth and dental composite resin with monocalcium phosphate MCP. *Rangsit Graduate Research Conference: RGRC*, 2020. pp. 2744-2757.
- Schumacher M. & Gelinsky M., 2015. Strontium modified calcium phosphate cements—approaches towards targeted stimulation of bone turnover. *Journal of Materials Chemistry B*. 3 (23), 4626-4640.
- Shah M., Paramshivam G., Mehta A., Singh S., Chugh A., Prashar A., et al., 2018. Comparative assessment of conventional and light-curable fluoride varnish in the prevention of enamel demineralization during fixed appliance therapy: a split-mouth randomized controlled trial. *European Journal of Orthodontics*. 40 (2), 132-139.
- Sharma S., Tandon P., Nagar A., Singh G. P., Singh A. & Chugh V. K., 2014. A comparison of shear bond strength of orthodontic brackets bonded with four different orthodontic adhesives. *Journal of orthodontic science*. 3 (2), 29.
- Shinohara M. S., Mario F., Schneider L. F. J., Ferracane J. L., Pereira P. N., Di Hipólito V., et al., 2009. Fluoride-containing adhesive: durability on dentin bonding. *Dental Materials*. 25 (11), 1383-1391.
- Shortall A., Palin W. & Burtscher P., 2008. Refractive index mismatch and monomer reactivity influence composite curing depth. *Journal of dental research*. 87 (1), 84-88.
- Shukla C., Maurya R., Singh V. & Tijare M., 2017. Evaluation of role of fixed orthodontics in changing oral ecological flora of opportunistic microbes in children and adolescent. *Journal of Indian Society of Pedodontics and Preventive Dentistry*. 35 (1), 34.
- Sideridou I., Tserki V. & Papanastasiou G., 2002. Effect of chemical structure on degree of conversion in light-cured dimethacrylate-based dental resins. *Biomaterials*. 23 (8), 1819-1829.
- Sifakakis I. & Eliades T., 2017. Adverse reactions to orthodontic materials. *Australian Dental Journal*. 62 20-28.
- Silva L. F. G. E., Thomaz E. B. a. F., Freitas H. V., Pereira A. L. P., Ribeiro C. C. C. & Alves C. M. C., 2016. Impact of malocclusion on the quality of life of Brazilian adolescents: a population-based study. *PloS one*. 11 (9), e0162715.
- Spanovic N., Bjelovucic R., Marovic D., Schmalz G., Gamulin O. & Tarle Z. J. D. M. J., 2019. Long-term water sorption and solubility of experimental bioactive composites based on amorphous calcium phosphate and bioactive glass. 2018-145.

- Sukontapatipark W., El - Agroudi M. A., Selliseth N. J., Thunold K. & Selvig K. A., 2001. Bacterial colonization associated with fixed orthodontic appliances. A scanning electron microscopy study. *The European Journal of Orthodontics*. 23 (5), 475-484.
- Sundararaj D., Venkatachalapathy S., Tandon A. & Pereira A., 2015. Critical evaluation of incidence and prevalence of white spot lesions during fixed orthodontic appliance treatment: A meta-analysis. *Journal of International Society of Preventive & Community Dentistry*. 5 (6), 433.
- Taghavi Bayat J., Huggare J., Mohlin B. & Akrami N., 2017. Determinants of orthodontic treatment need and demand: a cross-sectional path model study. *European Journal of Orthodontics*. 39 (1), 85-91.
- Tak M., Nagarajappa R., Sharda A. J., Asawa K., Tak A., Jalihal S., et al., 2013. Prevalence of malocclusion and orthodontic treatment needs among 12-15 years old school children of Udaipur, India. *European Journal of Dentistry*. 7 (S 01), S045-S053.
- Takamizawa T., Barkmeier W. W., Tsujimoto A., Berry T. P., Watanabe H., Erickson R. L., et al., 2016. Influence of different etching modes on bond strength and fatigue strength to dentin using universal adhesive systems. *Dental Materials*. 32 (2), e9-e21.
- Tristão S. K. P., Magno M. B., Pintor A. V. B., Christovam I. F., Ferreira D. M. T., Maia L. C., et al., 2020. Is there a relationship between malocclusion and bullying? A systematic review. *Progress in orthodontics*. 21 (1), 1-13.
- Tufekci E., Dixon J. S., Gunsolley J. & Lindauer S. J., 2011. Prevalence of white spot lesions during orthodontic treatment with fixed appliances. *The Angle Orthodontist*. 81 (2), 206-210.
- Van Strydonck D. A., Slot D. E., Van Der Velden U. & Van Der Weijden F., 2012. Effect of a chlorhexidine mouthrinse on plaque, gingival inflammation and staining in gingivitis patients: a systematic review. *Journal of Clinical Periodontology*. 39 (11), 1042-1055.
- Walters N. J., Xia W., Salih V., Ashley P. F. & Young A. M., 2016. Poly (propylene glycol) and urethane dimethacrylates improve conversion of dental composites and reveal complexity of cytocompatibility testing. *Dental Materials*. 32 (2), 264-277.
- Wang L.-J., Zhou X., Wang W., Tang F., Qi C.-L., Yang X., et al., 2011. Andrographolide inhibits oral squamous cell carcinogenesis through NF- κ B inactivation. *Journal of dental research*. 90 (10), 1246-1252.
- Xu H. H., Weir M. D. & Sun L., 2009. Calcium and phosphate ion releasing composite: effect of pH on release and mechanical properties. *Dental Materials*. 25 (4), 535-42.
- Xu Y.-T., Wu Q., Chen Y.-M., Smales R. J., Shi S.-Y. & Wang M.-T., 2015. Antimicrobial effects of a bioactive glass combined with fluoride or triclosan on *Streptococcus mutans* biofilm. *archives of oral biology*. 60 (7), 1059-1065.

- Yang S.-Y., Kim S.-H., Choi S.-Y. & Kim K.-M., 2016. Acid neutralizing ability and shear bond strength using orthodontic adhesives containing three different types of bioactive glass. *Materials*. 9 (3), 125.
- Yi J., Dai Q., Weir M. D., Melo M. A., Lynch C. D., Oates T. W., et al., 2019. A nano-CaF₂-containing orthodontic cement with antibacterial and remineralization capabilities to combat enamel white spot lesions. *Journal of Dentistry*. 89 103172.
- Zhang L., Weir M. D., Chow L. C., Reynolds M. A. & Xu H. H., 2016. Rechargeable calcium phosphate orthodontic cement with sustained ion release and re-release. *Scientific reports*. 6 (1), 1-11.
- Zope A., Zope-Khalekar Y., Chitko S. S., Kerudi V. V., Patil H. A., Bonde P. V., et al., 2016. Comparison of self-etch primers with conventional acid etching system on orthodontic brackets. *Journal of clinical and diagnostic research*. 10 (12), ZC19.

